EUROPEAN ORGANIZATION FOR NUCLEAR RESEARCH

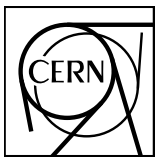

CERN-EP-2023-159
02 August 2023

Study of flavor dependence of the baryon-to-meson ratio in proton–proton collisions at $\sqrt{s} = 13$ TeV

ALICE Collaboration*

Abstract

The production cross sections of D^0 and Λ_c^+ hadrons originating from beauty-hadron decays (i.e. non-prompt) were measured for the first time at midrapidity ($|y| < 0.5$) by the ALICE Collaboration in proton–proton collisions at a center-of-mass energy $\sqrt{s} = 13$ TeV. They are described within uncertainties by perturbative QCD calculations employing the fragmentation fractions of beauty quarks to baryons measured at forward rapidity by the LHCb Collaboration. The $\mathrm{b\overline{b}}$ production cross section per unit of rapidity at midrapidity, estimated from these measurements, is $\mathrm{d}\sigma_{\mathrm{b\overline{b}}}/\mathrm{d}y|_{|y|<0.5} = 83.1 \pm 3.5(\mathrm{stat}) \pm 5.4(\mathrm{syst})^{+12.3}_{-3.2}(\mathrm{extrap})$ µb. The baryon-to-meson ratios are computed to investigate the hadronization mechanism of beauty quarks. The non-prompt $\Lambda_\mathrm{c}^+/\mathrm{D}^0$ production ratio has a similar trend to the one measured for the promptly produced charmed particles and to the p/π^+ and $\Lambda/\mathrm{K}^0_\mathrm{S}$ ratios, suggesting a similar baryon-formation mechanism among light, strange, charm, and beauty hadrons. The p_T-integrated non-prompt $\Lambda_\mathrm{c}^+/\mathrm{D}^0$ ratio is found to be significantly higher than the one measured in $\mathrm{e}^+\mathrm{e}^-$ collisions.

*See Appendix A for the list of collaboration members

1 Introduction

Measurements of open charm- and beauty-meson production in proton–proton (pp) collisions are successfully described by quantum chromodynamics (QCD) calculations based on the factorization of soft (non-perturbative) and hard (perturbative) processes [1–12]. Within the collinear factorization approach, the production cross sections of heavy-flavor hadrons are computed as the convolution of (i) the parton distribution functions (PDFs) of the incoming protons, (ii) the perturbative partonic cross section, and (iii) the fragmentation functions (FFs) describing the transition from the heavy quark to the hadron. The partonic cross section in these calculations is typically computed at next-to-leading order accuracy with all-order resummation of next-to-leading logarithms (e.g., FONLL [13–15] and GM-VFNS [16–21]), but recently calculations at next-to-next-to-leading order (NNLO) also became available [22]. The FFs are instead parametrized from measurements performed in e^+e^- or ep collisions [23], assuming that the hadronization process of charm and beauty quarks is independent of the collision system.

Recent measurements of charm baryon-to-meson production ratios and fragmentation fractions (i.e. the probability of charm quark to fragment into a specific hadron) at midrapidity in pp collisions at LHC energies showed significant deviations from the values measured at e^+e^- and ep colliders [24–32], demonstrating that the assumption of universality of the hadronization process across the collision systems has to be reconsidered. As reported in Ref. [30], the observed baryon-to-meson enhancement also leads to an increase of the derived $c\overline{c}$ production cross section at midrapidity compared to previous measurements, where prompt D-meson cross sections and fragmentation fractions from e^+e^- were used. Models based on the hadronization via coalescence, i.e. recombination of heavy and light quarks close in space and with similar velocity, are able to reproduce the magnitude as well as the $p_{\rm T}$ dependence of the measured $\Lambda_{\rm c}^+/{\rm D}^0$ ratio [33, 34]. An alternative explanation is provided by statistical hadronization models, if an augmented set of yet unobserved charm-baryon states predicted by the relativistic-quark model [35] and lattice QCD [36] is considered. Moreover, string fragmentation models including color-reconnection mechanisms beyond the leading-color (CLR-BLC) approximation introduce new topologies through the contributions of "junctions" that fragment into baryons, thus providing an augmented baryon production [37]. In the beauty sector, the measurements of $\Lambda_{\rm b}^0$-baryon production relative to that of B mesons at forward rapidity by the LHCb Collaboration show a modification of the fragmentation fractions among collision systems similar to that observed for charm quarks at midrapidity [38, 39]. However, the rapidity-dependent baryon-to-meson enhancement with respect to values measured at e^+e^- and ep colliders is still not fully understood and explored. Different enhancement was observed for the charm baryon-to-meson ratio between midrapidity and forward rapidity for $p_{\rm T} < 8$ GeV/c and for different colliding systems (i.e. pp, p–Pb) [27, 40, 41]. Beauty measurements at midrapidity are available only at high transverse momentum ($p_{\rm T} > 7$ GeV/c) [5, 42–48], hence a firm conclusion cannot be drawn.

In this article, the first measurements of the $p_{\rm T}$-differential and $p_{\rm T}$-integrated production cross sections of $\rm D^0$ mesons and $\Lambda_{\rm c}^+$ baryons at midrapidity ($|y| < 0.5$) originating from beauty-hadron decays (denoted as non-prompt) in pp collisions at a center-of-mass energy of $\sqrt{s} = 13$ TeV are reported. The differential measurements performed in $1 < p_{\rm T} < 24$ GeV/c and $2 < p_{\rm T} < 24$ GeV/c for $\rm D^0$ and $\Lambda_{\rm c}^+$ hadrons, respectively, are extrapolated down to $p_{\rm T} = 0$ to compute the $p_{\rm T}$-integrated production cross sections and compute the $\rm b\overline{b}$ production cross section at midrapidity. Finally, the non-prompt $\Lambda_{\rm c}^+/{\rm D}^0$ production ratio is compared with the production ratio of prompt $\Lambda_{\rm c}^+$ and $\rm D^0$, with the $\rm p/\pi^+$ and $\Lambda/{\rm K}_{\rm S}^0$ ratios, as well as with predictions based on the statistical hadronization model TAMU [49] or the PYTHIA 8 Monte Carlo (MC) generator [50] to investigate the hadronization mechanisms of beauty quarks into baryons and mesons.

2 Experimental apparatus and data sample

The description of the ALICE apparatus and of its performance is presented in detail in Refs. [51, 52]. The detectors used for the reconstruction of non-prompt charm-hadron decays are the Inner Tracking System (ITS), the Time Projection Chamber (TPC), and the Time-Of-Flight detector (TOF). These are located in the central barrel, which covers the pseudorapidity interval $|\eta| < 0.9$ inside a solenoid magnet of field strength $B = 0.5$ T. The ITS and the TPC are used for tracking charged particles and reconstructing particle decay vertices. Particle identification (PID) is performed via the measurement of the specific energy loss $\mathrm{d}E/\mathrm{d}x$ in the TPC and of the flight time with the TOF detector.

The data used for this analysis were collected during pp collisions at $\sqrt{s} = 13$ TeV, with a minimum bias (MB) trigger. The latter requires coincident signals in the two scintillator arrays covering the intervals $2.8 < \eta < 5.1$ (V0A) and $-3.7 < \eta < -1.7$ (V0C). Offline selections were applied to remove background from beam–gas collisions, as described in Ref. [27]. Only events with a primary vertex reconstructed within ± 10 cm from the nominal interaction point along the beam line were analyzed. Events with multiple primary vertices were rejected in order to remove collision pileup in the same bunch crossing. The remaining undetected pileup is negligible. The selected events correspond to an integrated luminosity $\mathscr{L}_{\mathrm{int}} = 31.9 \pm 0.5\ \mathrm{nb}^{-1}$ [53].

3 Data analysis

3.1 D^0 and Λ_{c}^+ raw yields

The D^0 meson, Λ_{c}^+ baryon, and their charge conjugates were reconstructed via the hadronic decay channels $\mathrm{D}^0 \to \mathrm{K}^-\pi^+$ (branching ratio $\mathrm{BR} = 3.95 \pm 0.03\%$), $\Lambda_{\mathrm{c}}^+ \to \mathrm{pK}_{\mathrm{S}}^0$ ($\mathrm{BR} = 1.59 \pm 0.08\%$, followed by $\mathrm{K}_{\mathrm{S}}^0 \to \pi^+\pi^-$ with a BR of $69.20 \pm 0.05\%$), and $\Lambda_{\mathrm{c}}^+ \to \mathrm{pK}^-\pi^+$ ($\mathrm{BR} = 6.28 \pm 0.32\%$) [54]. The D^0-meson and Λ_{c}^+-baryon candidates were reconstructed by combining pairs or triplets of tracks reconstructed with the proper charge, while for the $\Lambda_{\mathrm{c}}^+ \to \mathrm{pK}_{\mathrm{S}}^0$ channel the V-shaped decay of the $\mathrm{K}_{\mathrm{S}}^0$ meson into two pion-track candidates was combined with a proton-track candidate, using a Kalman-Filter vertexing algorithm [55]. All daughter tracks were required to be reconstructed within $|\eta| < 0.8$ and to have at least 70 reconstructed space points in the TPC. For all decay products, at least one cluster was required in either of the two SPD layers. As a consequence of these track-quality selections, the detector acceptance for the candidates falls steeply to zero for $|y| \approx 0.5$ at $p_{\mathrm{T}} \approx 0$ and at $|y| \approx 0.8$ for $p_{\mathrm{T}} > 5$ GeV/c. Thus, a fiducial-acceptance selection $|y| < y_{\mathrm{fid}}(p_{\mathrm{T}})$ was applied, increasing from 0.5 at $p_{\mathrm{T}} = 0$ to the maximum value of 0.8 at $p_{\mathrm{T}} \geq 5$ GeV/c.

A multi-class classification approach based on Boosted Decision Trees (BDT) algorithms provided by the XGBOOST [56, 57] library, was used to simultaneously reduce the combinatorial background, and to separate the prompt and non-prompt components for D^0 mesons and Λ_{c}^+ baryons. Indeed, the inclusive sample of D^0 and Λ_{c}^+ is dominated by the prompt hadrons and the non-prompt ones are a small fraction which can be enhanced exploiting the larger displacement due to the beauty-hadron decay topology. Signal samples of prompt and non-prompt candidates for the BDT training were obtained from MC simulations produced with the PYTHIA 8.243 [50] event generator with the Monash 2013 tune [58]. The generated particles were propagated through the ALICE apparatus using the GEANT3 transport code [59]. Background samples were extracted from the candidate invariant-mass distributions inside the window of $5\sigma < |\Delta M| < 9\sigma$ in data, where ΔM is the difference between the candidate invariant mass and the D^0 (Λ_{c}^+) mass, and σ is the invariant-mass resolution. Loose selections on the decay kinematics, the decay topology, and the PID of the decay particles were applied to the candidates before the training. The BDTs were trained in each p_{T} interval using different variables related to the displaced decay-vertex topology and the PID of the decay tracks, similarly as described in Refs. [2, 60]. The BDT outputs are related to the candidate's probability to be either prompt or non-prompt D^0 (Λ_{c}^+) meson (baryon) or combinatorial background. Selections on the BDT output probabilities of being background and non-

prompt were optimized to obtain a high non-prompt D^0 and Λ_c^+ fractions (i.e. $\geq 60\%$ in each p_T interval) while maintaining a reliable signal extraction. The sample of candidates passing the BDT selection is denoted in the following as non-prompt enhanced sample. Based on the selections on the BDT outputs, samples dominated by non-prompt (prompt) candidates were selected by requiring low BDT probability for a candidate to be combinatorial background and a high BDT probability to be non-prompt (prompt).

The D^0-meson and Λ_c^+-baryon raw yields were extracted via binned maximum-likelihood fits to the candidate invariant-mass distributions. The fitting function was composed of a Gaussian term to model the signal and an exponential or polynomial function to model the background. In the case of D^0 mesons, an additional term was added for the contribution of signal candidates with the wrong K–π mass assignment (reflections), parameterized from simulated candidates [1]. To improve the stability of the fits, the widths of the signal peaks were fixed to the values extracted from the fits of the invariant-mass distributions in the prompt enhanced sample, given the naturally larger abundance of prompt compared to non-prompt candidates. Examples of invariant-mass fits with different contributions of signal from beauty-hadron decays in the $2 < p_\mathrm{T} < 4$ GeV/c interval are shown in Fig. 1 for D^0 (top row), $\Lambda_\mathrm{c}^+ \rightarrow \mathrm{pK}_\mathrm{S}^0$ (middle row), and $\Lambda_\mathrm{c}^+ \rightarrow \mathrm{pK}^-\pi^+$ (bottom row). The blue solid curves show the total fit function, the red dashed curves show the combinatorial-background contribution, and the green solid lines represent the reflection contribution only for D^0. The fits to the invariant-mass distributions of non-prompt (prompt) enhanced samples are shown in each right (left) panel, indicating the corresponding selection applied on the BDT output score related to the probability to be a non-prompt (prompt) charm hadron.

3.2 Yield corrections and non-prompt fraction estimate

The non-prompt D^0 and Λ_c^+ p_T-differential cross sections were obtained in the rapidity interval $|y| < 0.5$ as

$$\frac{\mathrm{d}\sigma^{\Lambda_\mathrm{c}^+(\mathrm{D}^0)}}{\mathrm{d}p_\mathrm{T}\mathrm{d}y} = \frac{1}{\mathrm{BR}} \times \frac{1}{2c_{\Delta y}(p_\mathrm{T})\Delta p_\mathrm{T}} \times \frac{f_{\text{non-prompt}} \times N_\mathrm{raw}}{(\mathrm{Acc} \times \varepsilon)_{\text{non-prompt}}} \times \frac{1}{\mathscr{L}_\mathrm{int}}, \tag{1}$$

where N_raw is the raw yield (sum of particles and antiparticles), $c_{\Delta y}(p_\mathrm{T})$ and Δp_T represent the width of the rapidity and transverse momentum intervals respectively, BR is the branching ratio of the considered decay mode, the factor of 2 is introduced to obtain the average of particle and antiparticle yields, $f_{\text{non-prompt}}$ is the fraction of non-prompt hadrons in the raw yield, $(\mathrm{Acc} \times \varepsilon)_{\text{non-prompt}}$ is the product of the geometrical acceptance and the reconstruction and selection efficiency for non-prompt hadrons, which increases with p_T from 5% to 25% depending on the BDT selections and decay channel for Λ_c^+ (5% to 40% for D^0), and $\mathscr{L}_\mathrm{int}$ is the integrated luminosity. The correction factors $(\mathrm{Acc} \times \varepsilon)$ for the detector acceptance and the signal reconstruction and selection efficiency were determined using the aforementioned MC simulations.

A data-driven procedure based on the construction of data samples with different abundances of prompt and non-prompt candidates was used to estimate the fraction $f_{\text{non-prompt}}$ of non-prompt D^0 and non-prompt Λ_c^+ hadrons. A set of raw yields (Y_i) can be obtained by varying the selection on the BDT output, which is related to the candidate's probability to be a non-prompt D^0 meson or a non-prompt Λ_c^+ baryon. These raw yields are sensitive to the corresponding $(\mathrm{Acc} \times \varepsilon)$ of prompt and non-prompt D^0 or Λ_c^+ hadrons as follows

$$(\mathrm{Acc} \times \varepsilon)_\mathrm{i}^{\text{prompt}} \times N_{\text{prompt}} + (\mathrm{Acc} \times \varepsilon)_\mathrm{i}^{\text{non-prompt}} \times N_{\text{non-prompt}} - Y_\mathrm{i} = \delta_\mathrm{i}, \tag{2}$$

where δ_i represents a residual that accounts for the equation not holding exactly due to the uncertainties of Y_i, $(\mathrm{Acc} \times \varepsilon)_\mathrm{i}^{\text{non-prompt}}$, and $(\mathrm{Acc} \times \varepsilon)_\mathrm{i}^{\text{prompt}}$. In the case of $n \geq 2$ sets, a χ^2 function can be defined

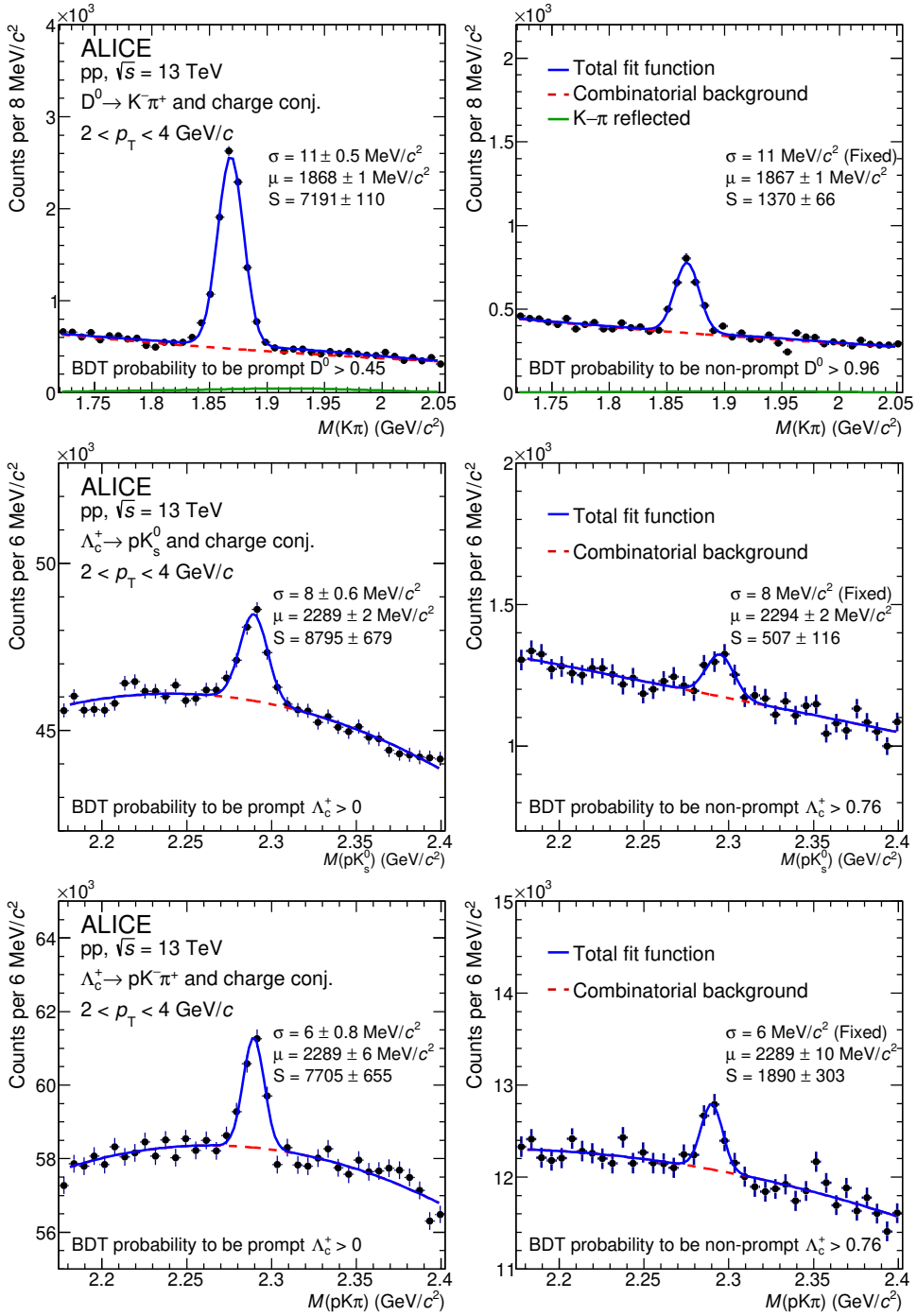

Figure 1: Invariant-mass distributions of the D^0- and Λ_c^+-hadron candidates and their charge conjugates produced in pp collisions at $\sqrt{s} = 13$ TeV and reconstructed at midrapidity, shown in a selected p_T range. The values for the Gaussian mean μ, width σ, and raw yield S are reported. Top row: $D^0 \to K^-\pi^+$ meson candidates measured in the $2 < p_T < 4$ GeV/c interval. Middle row: $\Lambda_c^+ \to pK_S^0$ baryon candidates measured in the $2 < p_T < 4$ GeV/c interval. Bottom row: $\Lambda_c^+ \to pK^-\pi^+$ baryon candidates measured in the $2 < p_T < 4$ GeV/c interval. The corresponding BDT probability minimum threshold for the candidate selection is reported. The left (right) column corresponds to the prompt (non-prompt) D^0- and Λ_c^+- hadron candidates enriched sample.

based on Eq. 2, which can be minimized to obtain the corrected yields of prompt (N_{prompt}) and non-prompt ($N_{\text{non-prompt}}$) Λ_c^+ (D^0) hadrons as explained in Ref. [2]. One of the n sets with a high non-

prompt component (larger than 50%) was selected as a working point (default), and the corresponding $f_{\text{non-prompt,default}}$ fraction (more details in Ref. [2]) can be calculated as

$$f_{\text{non-prompt,default}} = \frac{(\text{Acc} \times \varepsilon)^{\text{non-prompt}}_{\text{default}} \times N_{\text{non-prompt}}}{(\text{Acc} \times \varepsilon)^{\text{non-prompt}}_{\text{default}} \times N_{\text{non-prompt}} + (\text{Acc} \times \varepsilon)^{\text{prompt}}_{\text{default}} \times N_{\text{prompt}}}. \quad (3)$$

Figure 2 shows an example of raw-yield distribution as a function of the BDT-based selection employed in the minimization procedure for $\mathrm{D^0}$ in $2 < p_{\mathrm{T}} < 4$ GeV/c (top left panel), $\Lambda_{\mathrm{c}}^{+} \to \mathrm{pK^-}\pi^+$ in $4 < p_{\mathrm{T}} < 6$ GeV/c (top right panel), and $\Lambda_{\mathrm{c}}^{+} \to \mathrm{pK^0_S}$ in $6 < p_{\mathrm{T}} < 8$ GeV/c (bottom left panel). The black markers are the measured raw yields corresponding to a selection on the BDT output related to the candidate's probability of being a non-prompt $\mathrm{D^0}$ (Λ_{c}^{+}) meson (baryon). The leftmost data point of each distribution corresponds to the loosest applied selection, while the rightmost one corresponds to the tightest selection, which preferentially selects non-prompt candidates. The prompt and non-prompt components, obtained for each BDT-based selection from the minimization procedure as $(\text{Acc} \times \varepsilon)^{\text{prompt}}_{\text{i}} \times N_{\text{prompt}}$ and $(\text{Acc} \times \varepsilon)^{\text{non-prompt}}_{\text{i}} \times N_{\text{non-prompt}}$, are represented by the red and blue filled histograms, respectively, while their sum is reported by the green histogram. The $f_{\text{non-prompt}}$ fractions obtained for $\mathrm{D^0}$, $\Lambda_{\mathrm{c}}^{+} \to \mathrm{pK^-}\pi^+$, and $\Lambda_{\mathrm{c}}^{+} \to \mathrm{pK^0_S}$, computed for the default selections with the formula in Eq. 3 are reported as a function of p_{T} in the bottom right panel of Fig. 2.

4 Systematic uncertainties

The systematic uncertainties of the non-prompt Λ_{c}^{+} and $\mathrm{D^0}$ cross sections were studied for the different decay channels, which depend on p_{T}. The contributions from the raw-yield extraction were evaluated by repeating the invariant-mass fits, varying the fit interval, the functional form of the background fit function, and the width of the Gaussian function used to model the signal peaks. The latter was varied within the uncertainties obtained from the fits of the invariant-mass distributions of the prompt enhanced sample. The relative uncertainty from this contribution varies in the range 1–3% for $\mathrm{D^0}$ and 4–11% for Λ_{c}^{+}. The uncertainties of the track reconstruction efficiency were estimated by considering the uncertainty due to track quality selections and the uncertainty due to the TPC–ITS track matching efficiency as discussed in Ref. [2]. It ranges from 3.5% to 5% for $\mathrm{D^0}$ and from 4% to 7% for Λ_{c}^{+}. The systematic uncertainties of the non-prompt fractions were evaluated by varying the configuration and the number of BDT selections employed in the data-driven method and amounts to 2–3% for $\mathrm{D^0}$ and 5–9% for Λ_{c}^{+}. The selection efficiency uncertainties, ranging from 2% to 4% for $\mathrm{D^0}$ and 4% to 10% for Λ_{c}^{+}, were studied by repeating the analyses using different BDT working points. The systematic uncertainties of the PID selection efficiency were found to be negligible, similar to what observed for prompt charm hadrons [60]. The systematic effects due to a possible difference between the real and simulated charm and beauty hadron p_{T} spectra, were estimated by evaluating the selection efficiency after reweighting the p_{T} shape from the PYTHIA 8.243 event generator to match the one from FONLL calculations [13–15] for prompt and non-prompt $\mathrm{D^0}$. For the Λ_{c}^{+} the reweighting was defined to match the p_{T} shape of $\mathrm{D^0}$ and B mesons from FONLL multiplied by the $\Lambda_{\mathrm{c}}^{+}/\mathrm{D^0}$ yield ratio from ALICE [27] and the $\Lambda_{\mathrm{b}}^{0}/\mathrm{B}$ yield ratio from LHCb [39], respectively. The weights were applied to the p_{T} distributions for prompt hadrons and to the mother beauty-hadron particles in the case of non-prompt hadrons. The systematic uncertainty from this contribution varies in the range 1–4% for $\mathrm{D^0}$ and 4–5% for Λ_{c}^{+}. In addition, the imperfect apparatus material budget description in the MC simulation, particularly relevant for the effects of the absorption of protons, might result in a bias in the estimation of the Λ_{c}^{+} efficiencies. It was evaluated by comparing the corrected yields of charged pions, kaons, and protons using a standard MC production and one with the material budget increased artificially by 10%. The assigned systematic uncertainty is 2%. Further p_{T}-independent uncertainties from the BR [61] and the luminosity [53] were considered. The total uncertainties, 5–8% for $\mathrm{D^0}$ and 12–17% for Λ_{c}^{+}, were calculated as the quadratic sum of the contributions of the different sources.

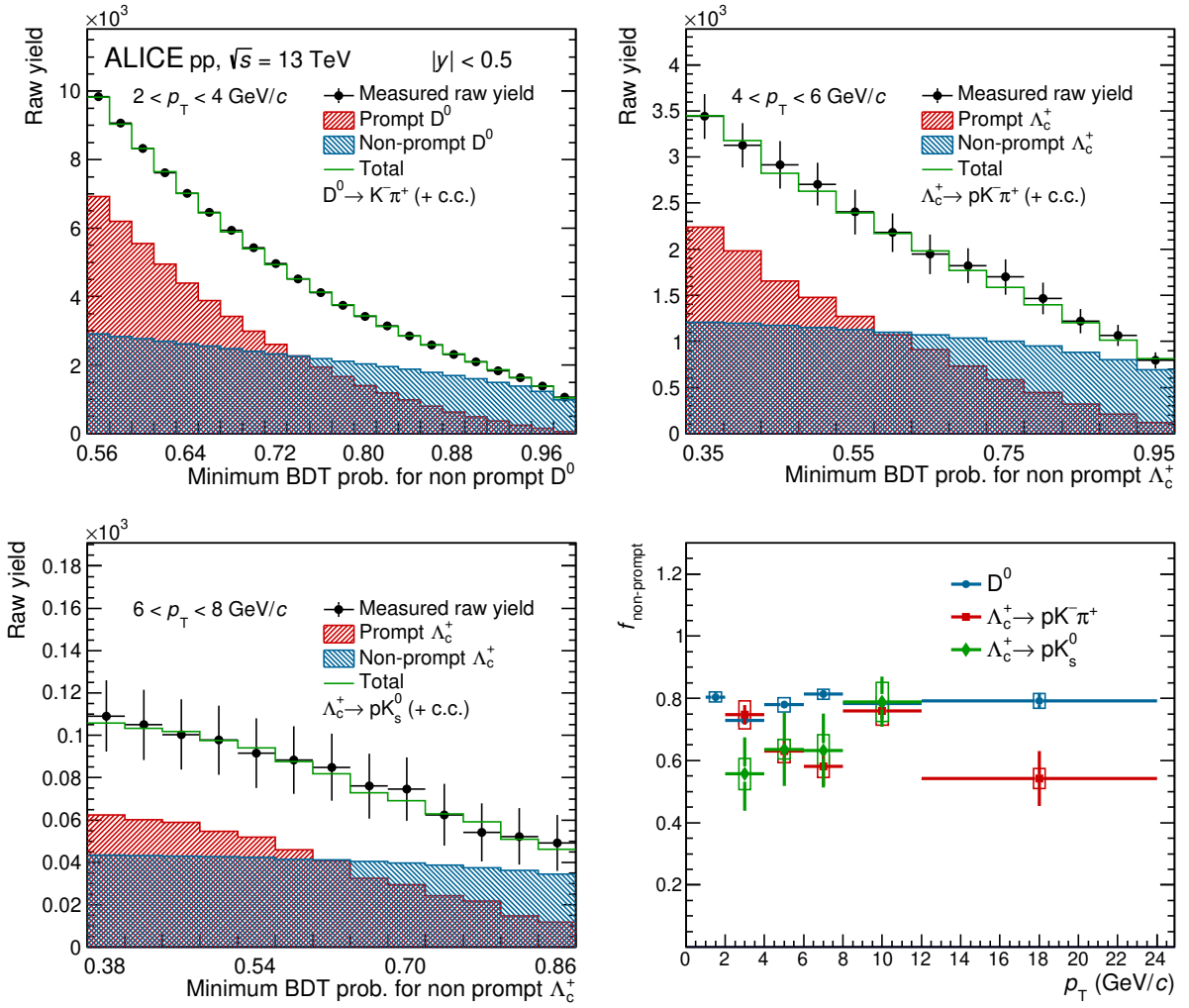

Figure 2: Raw-yield distribution as a function of the BDT-based selection employed in the χ^2-minimization procedure adopted for the determination of $f_{\text{non-prompt}}$ of $\mathrm{D^0}$ in $2 < p_{\mathrm{T}} < 4$ GeV/c (top left panel), $\Lambda_{\mathrm{c}}^{+} \rightarrow \mathrm{pK^{-}\pi^{+}}$ in $4 < p_{\mathrm{T}} < 6$ GeV/c (top right panel), and $\Lambda_{\mathrm{c}}^{+} \rightarrow \mathrm{pK_S^0}$ in $6 < p_{\mathrm{T}} < 8$ GeV/c (bottom left panel). Bottom right panel: $f_{\text{non-prompt}}$ fraction as function as p_{T} obtained for the set of selection criteria adopted in the analysis of for non-prompt $\mathrm{D^0}$, $\Lambda_{\mathrm{c}}^{+} \rightarrow \mathrm{pK^{-}\pi^{+}}$, and $\Lambda_{\mathrm{c}}^{+} \rightarrow \mathrm{pK_S^0}$ hadrons.

5 Results

5.1 Production cross sections

The p_{T}-differential production cross sections of non-prompt Λ_{c}^{+} baryons and $\mathrm{D^0}$ mesons are shown in Fig. 3. The non-prompt Λ_{c}^{+} cross section was obtained by computing a weighted average of the results from the analyses of the $\Lambda_{\mathrm{c}}^{+} \rightarrow \mathrm{pK_S^0}$ and $\Lambda_{\mathrm{c}}^{+} \rightarrow \mathrm{pK^{-}\pi^{+}}$ decay channels, using the inverse of the quadratic sum of the relative statistical and uncorrelated systematic uncertainties as weights. The systematic uncertainties related to the tracking, luminosity, and generated p_{T} spectrum in the MC simulations are treated as correlated between the two decay channels, the uncertainty of the branching ratios as partially correlated as described in Ref. [54], while all the other sources of systematic uncertainties are considered uncorrelated. The data points are compared with theoretical models based on the B-meson cross section predicted by FONLL calculations in the left panel and to the TAMU statistical hadronization model [49] in the right panel. In the FONLL-based predictions, the beauty-quark fragmentation fraction to B mesons, $f(\mathrm{b} \rightarrow \mathrm{B})$, was taken from $\mathrm{e^{+}e^{-}}$ collisions [54]. For the Λ_{b}^{0} baryon, $f(\mathrm{b} \rightarrow \mathrm{B})_{\mathrm{e^{+}e^{-}}} \times$

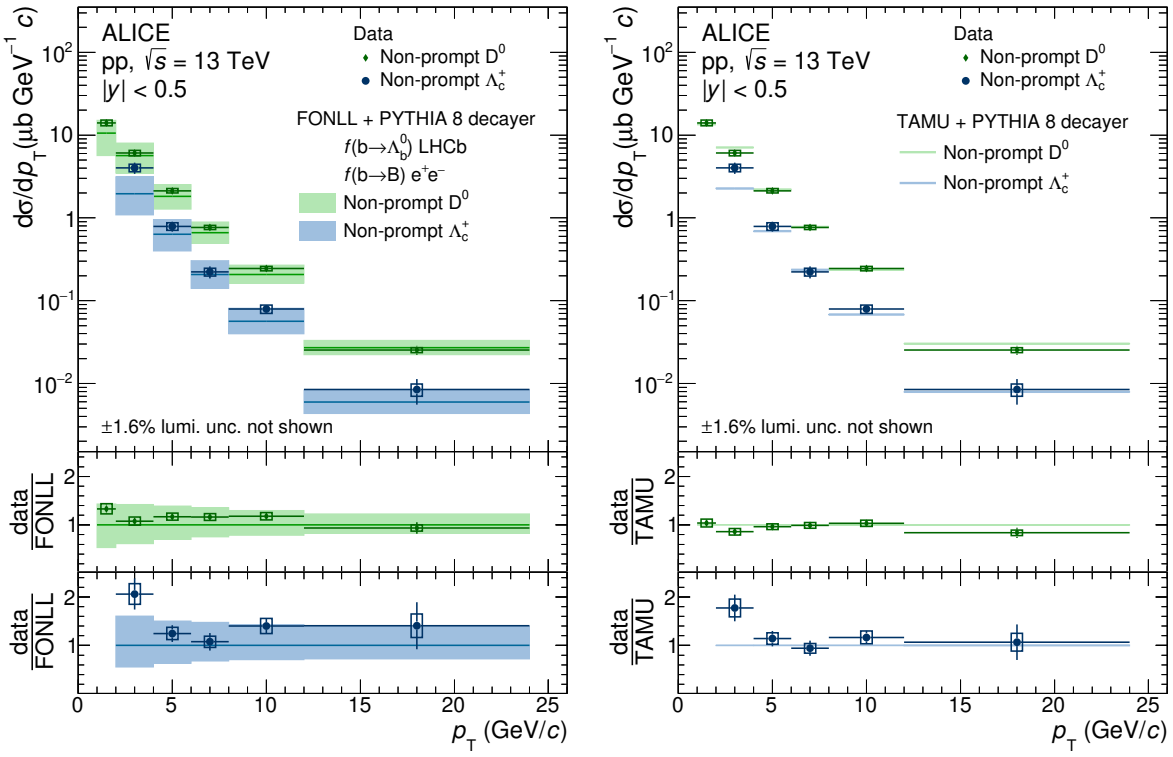

Figure 3: p_{T}-differential production cross sections of non-prompt D^0 and Λ_{c}^+ hadrons in pp collisions at $\sqrt{s} = 13$ TeV compared with predictions obtained with FONLL calculations [13–15] adopting $f(\mathrm{b} \to \mathrm{B})$ and $f(\mathrm{b} \to \Lambda_{\mathrm{b}}^0)$ fragmentation fractions measured in $\mathrm{e}^+\mathrm{e}^-$ collisions [61] and LHCb Collaboration [39] (left panel) and the TAMU model [49] (right panel) combined with PYTHIA 8 [50, 58] for the $\mathrm{h_b} \to \mathrm{h_c} + \mathrm{X}$ decay kinematics.

$(f(\mathrm{b} \to \Lambda_{\mathrm{b}}^0)/f(\mathrm{b} \to \mathrm{B}))_{\mathrm{LHCb}}$ was used, where the p_{T}-differential ratio Λ_{b}^0 /B was measured by the LHCb Collaboration in pp collisions [39]. It has to be noted that the usage of the p_{T}-differential fragmentation fractions ratio $(f(\mathrm{b} \to \Lambda_{\mathrm{b}}^0)/f(\mathrm{b} \to \mathrm{B}))_{\mathrm{LHCb}}$ combined with the $f(\mathrm{b} \to \mathrm{B})$ from $\mathrm{e}^+\mathrm{e}^-$ collisions enlarges the total beauty production cross section compared to the one predicted by FONLL calculations. In the TAMU model instead, the branching fractions of beauty quarks to the different hadron species are assumed to follow the relative thermal densities calculated with the statistical hadronization model and an enriched set of heavy-flavor hadron states is obtained from the relativistic-quark model [35]. The p_{T} distribution is obtained from the one of beauty quarks, convoluted to the fragmentation functions as implemented in FONLL calculations. In this case, the $\mathrm{b\overline{b}}$ production cross section at midrapidity is a parameter of the model, fixed to $\mathrm{d}\sigma_{\mathrm{b\overline{b}}}/\mathrm{d}y|_{y=0} = 85.3$ μb.

The resulting beauty-hadron cross sections of both models were then folded with the $\mathrm{h_b} \to \mathrm{h_c} + \mathrm{X}$ decay kinematics (where $\mathrm{h_c}$ and $\mathrm{h_b}$ denote a generic hadron species containing either a charm or beauty quark) and branching ratios provided by the PYTHIA 8 decayer, in order to obtain the non-prompt D^0 and Λ_{c}^+ cross sections. In the left panel, the uncertainties in the model are those of the FONLL calculation, which arise from the choice of the normalization and factorization scales, and the mass of the beauty quark, combined with the uncertainties of the CTEQ6.6 PDFs. The non-prompt D^0 cross section is in agreement with FONLL + PYTHIA 8 and TAMU + PYTHIA 8 predictions over the whole p_{T} range, while the non-prompt Λ_{c}^+ cross section shows a hint of underestimation at low p_{T} ($2 < p_{\mathrm{T}} < 4$ GeV/c) by both models.

The measured visible cross sections of non-prompt Λ_{c}^+ and D^0 hadrons were computed by integrating the measured p_{T}-differential cross sections in the measured p_{T} range. All the systematic uncertainties

were propagated as fully correlated among the measured $p_{\rm T}$ intervals, except for the raw-yield extraction uncertainty. As the $p_{\rm T}$-differential cross sections predicted by FONLL + PYTHIA 8 were found to be compatible with the measurements, they were assumed to provide an accurate description of the $p_{\rm T}$ shape also outside of the measured $p_{\rm T}$ range. Therefore, the visible cross section was then extrapolated to the full $p_{\rm T}$ range, using an extrapolation factor computed as the ratio of the $p_{\rm T}$-integrated cross sections predicted by FONLL + PYTHIA 8 integrated over $p_{\rm T} > 0$ and that in the measured $p_{\rm T}$ interval. The systematic uncertainty of the extrapolation factors was computed considering (i) the FONLL uncertainties, (ii) the $f(\mathrm{b} \to \mathrm{h_b})$ fragmentation fractions uncertainties, and (iii) the branching ratios uncertainties of the $\mathrm{h_b} \to \mathrm{h_c} + \mathrm{X}$ decays. The second source was estimated by using different sets of beauty fragmentation fractions (from $\mathrm{e^+e^-}$, $\mathrm{p\overline{p}}$ collisions [54], or those measured by LHCb [39]), while for the third one the branching ratios implemented in PYTHIA 8 were reweighted in order to reproduce the measured values reported in Ref [54]. The resulting extrapolation factors are $\alpha^{\rm D^0}_{\rm extrap} = 1.241^{+0.009}_{-0.047}$ and $\alpha^{\Lambda_{\rm c}^+}_{\rm extrap} = 1.847^{+0.108}_{-0.152}$ for $\mathrm{D^0}$ mesons and $\Lambda_{\rm c}^+$ baryons, respectively. The $p_{\rm T}$-integrated cross sections are reported in Table 1 and compared to FONLL + PYTHIA 8 calculations, which describe the measurements within the uncertainties.

Similarly, the $\mathrm{b\overline{b}}$ production cross section per unit of rapidity at midrapidity was obtained summing the visible cross sections previously computed and then using an extrapolation factor to account for the unmeasured $p_{\rm T}$ regions and hadrons. This factor was computed as the ratio of the beauty cross section and the visible cross section of a non-prompt charm hadron, estimated with FONLL + PYTHIA 8 as follows

$$\alpha^{\rm b\overline{b}}_{\rm extrap} = \frac{{\rm d}\sigma^{\rm FONLL}_{\rm b\overline{b}}/{\rm d}y|_{|y|<0.5}}{{\rm d}\sigma^{\rm FONLL+PYTHIA\ 8}_{\rm h_c \leftarrow b}/{\rm d}y|_{|y|<0.5}(p_{\rm T}^{\rm min\ h_c} < p_{\rm T} < p_{\rm T}^{\rm max\ h_c})}. \quad (4)$$

The extrapolation factor for the $\mathrm{D^0}$ meson was found to be $\alpha^{\rm b\overline{b},\ D^0}_{\rm extrap} = 2.106^{+0.366}_{-0.014}$, while the one for $\Lambda_{\rm c}^+$ baryons $\alpha^{\rm b\overline{b},\ \Lambda_c^+}_{\rm extrap} = 10.98^{+0.87}_{-1.34}$. The systematic uncertainty of the extrapolation factor includes the same sources considered for the extrapolation of the single-hadron production cross sections. In addition, a correction due to the difference between the rapidity distributions of beauty quarks and beauty hadrons, and between the $\mathrm{b\overline{b}}$ pairs and beauty quarks was applied. The first factor was evaluated to be unity in the relevant rapidity range based on FONLL calculations with 1% uncertainties evaluated from the difference between FONLL and PYTHIA 8. The second correction factor is the ratio $({\rm d}\sigma_{\rm b\overline{b}}/{\rm d}y)/({\rm d}\sigma_{\rm b}/{\rm d}y) = 1.06 \pm 0.01$ in $|y| < 0.5$, which was estimated from POWHEG simulations [62]. The uncertainty was assigned by varying the factorization and renormalization scales in the POWHEG calculation and using the CT10NLO [63] and CT14NLO [64] PDFs, alternatively to the default one (CTEQ6.6). The ${\rm d}\sigma_{\rm b\overline{b}}/{\rm d}y$ was computed separately from the measurements of non-prompt $\mathrm{D^0}$ and $\Lambda_{\rm c}^+$ hadrons were then averaged using the inverse of the quadratic sum of the absolute statistical and uncorrelated systematic uncertainties as weights. The systematic uncertainties related to the tracking uncertainty and the extrapolation uncertainties related to FONLL and the beauty fragmentation fractions were treated as fully correlated among the two hadron species, while all the other sources as uncorrelated. The resulting $\mathrm{b\overline{b}}$ production cross section per unit of rapidity at midrapidity is compatible with the predictions from FONLL and NNLO

Table 1: Production cross sections at midrapidity per unit of rapidity $({\rm d}\sigma/{\rm d}y)_{|y|<0.5}$ in pp collisions at $\sqrt{s} = 13$ TeV of non-prompt $\Lambda_{\rm c}^+$ and $\mathrm{D^0}$ hadrons and $\mathrm{b\overline{b}}$ pairs $({\rm d}\sigma_{\rm b\overline{b}}/{\rm d}y)_{|y|<0.5}$ compared to pQCD calculations [13–15, 22].

	Measurement (μb)	FONLL (μb) [13–15]	NNLO (μb) [22]
$\mathrm{D^0}$	$41.3 \pm 1.5({\rm stat}) \pm 2.9({\rm syst})^{+0.3}_{-1.6}({\rm extrap})$	34 ± 14	-
$\Lambda_{\rm c}^+$	$19.1 \pm 2.3({\rm stat}) \pm 1.7({\rm syst})^{+1.0}_{-1.5}({\rm extrap})$	11^{+7}_{-5}	-
$\mathrm{b\overline{b}}$	$83.1 \pm 3.5({\rm stat}) \pm 5.4({\rm syst})^{+12.3}_{-3.2}({\rm extrap})$	65^{+28}_{-26}	72^{+22}_{-20}

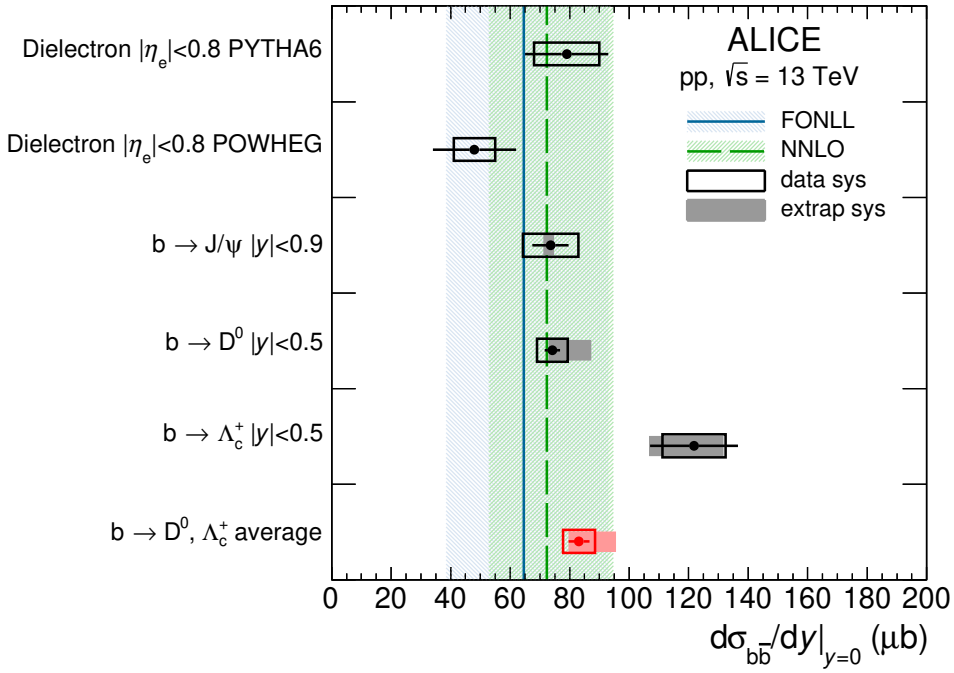

Figure 4: Beauty production cross section per rapidity unit at midrapidity obtained from from dielectron [66] and non-prompt J/ψ [3], D^0, and Λ_c^+ hadrons measured in pp collisions at $\sqrt{s} = 13$ TeV compared to FONLL [13–15] and NNLO [22] predictions. The average $\mathrm{d}\sigma_{\mathrm{b\bar{b}}}/\mathrm{d}y$ of the estimates from the D^0 and Λ_c^+ hadrons is also reported.

calculations, as reported in Table 1. The NNLO predictions are however closer to the measurement and have smaller uncertainties than the FONLL ones, as expected by the higher perturbative accuracy. The measurement is also compatible with previous estimates based on the measurements of dielectrons [65, 66] and non-prompt J/ψ mesons [3].

Figure 4 shows the $\mathrm{b\bar{b}}$ production cross section per unit rapidity at midrapidity estimated from the production cross sections of non-prompt D^0 and Λ_c^+ hadrons in pp collisions at $\sqrt{s} = 13$ TeV compared to the previous values based on dielectron and non-prompt J/ψ-meson measurements. The experimental results are also compared with the predictions provided by FONLL and NNLO perturbative QCD calculations.

5.2 Baryon-to-meson ratios

The ratio of the p_T-differential production cross sections of non-prompt Λ_c^+ and D^0 hadrons is shown in Fig. 5. In the left panel, the data are compared with theoretical predictions obtained with FONLL calculations [13–15] and PYTHIA 8 [50, 58] for the description of the decay kinematics and branching ratios. They are obtained using fragmentation fractions from $\mathrm{e^+e^-}$ collisions [61] for the B mesons and the $f(\mathrm{b} \to \Lambda_\mathrm{b}^0)/f(\mathrm{b} \to \mathrm{B})$ fragmentation fraction ratio measured by the LHCb Collaboration [39]. The contributions of non-prompt Λ_c^+ baryons originating from B mesons and Λ_b^0 baryons are reported separately to show that the largest contribution is represented by the beauty baryons, while the B mesons contribute only marginally to the non-prompt Λ_c^+ production cross section. Hence, it is possible to inquire the hadronization of beauty quarks into Λ_b^0 baryons through the non-prompt Λ_c^+. In the right panel of the same figure the data are compared with the p_T-differential ratio between prompt Λ_c^+ and D^0 hadrons. The two measurements are compatible in their common p_T range, with a tension of less than two standard deviations in $2 < p_\mathrm{T} < 4$ GeV/c, where the ratio of non-prompt hadrons is higher than the one of promptly produced hadrons. The experimental data are also compared to the predictions obtained

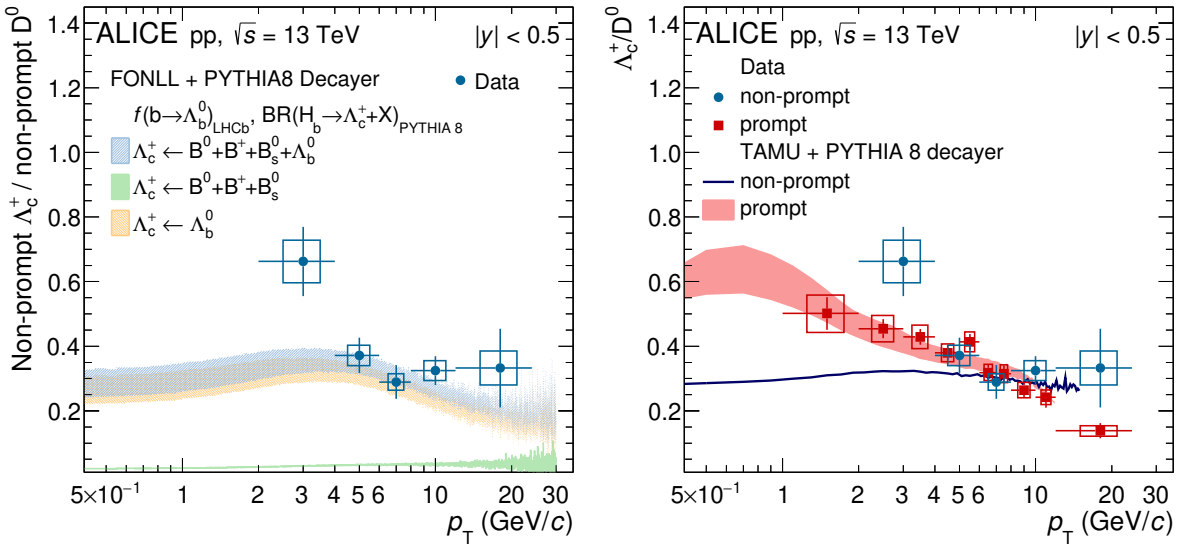

Figure 5: Left: p_{T}-differential ratios of non-prompt Λ_{c}^{+}- and D^{0}-hadron cross sections compared with predictions obtained with FONLL calculations [13–15] and PYTHIA 8 [50, 58] for the $\mathrm{h_b} \rightarrow \mathrm{h_c} + \mathrm{X}$ decay kinematics. The contributions from beauty mesons and from the Λ_{b}^{0} baryon are depicted separately. Right: p_{T}-differential ratios of prompt [27] and non-prompt Λ_{c}^{+}- and D^{0}-hadron cross sections compared with predictions obtained with the TAMU model [36, 49] and PYTHIA 8 for the $\mathrm{h_b} \rightarrow \mathrm{h_c} + \mathrm{X}$ decay kinematics.

with the TAMU model combined with PYTHIA 8 to describe the $\mathrm{h_b} \rightarrow \mathrm{h_c} + \mathrm{X}$ decay kinematics, in the case of non-prompt production. The prediction for prompt charm hadrons has an error band representing the uncertainty on the BR of excited charm baryons decaying into Λ_{c}^{+}, not included in the one for non-prompt hadrons. The measured non-prompt $\Lambda_{\mathrm{c}}^{+}/\mathrm{D}^{0}$ ratio is rather well described for $p_{\mathrm{T}} > 4$ GeV/c given the current uncertainties, while it is underestimated for $2 < p_{\mathrm{T}} < 4$ GeV/c. The prompt charm and beauty ratios are described by the TAMU calculations within the uncertainties for the whole measured p_{T} interval.

Figure 6 shows the p_{T}-differential non-prompt $\Lambda_{\mathrm{c}}^{+}/\mathrm{D}^{0}$ yield ratio at midrapidity ($|y| < 0.5$) in pp collisions at $\sqrt{s} = 13$ TeV compared with the measurements of prompt $\Lambda_{\mathrm{c}}^{+}/\mathrm{D}^{0}$ [27], $\Lambda/\mathrm{K}_{\mathrm{S}}^{0}$ [67], and p/π^{+} [67] ratios at the same energy and rapidity interval, and with the $\Lambda_{\mathrm{b}}^{0}/(\mathrm{B}^{0}+\mathrm{B}^{+})$ yield ratio measured by LHCb at forward rapidity ($2.5 < y < 4$). The $\Lambda_{\mathrm{b}}^{0}/(\mathrm{B}^{0}+\mathrm{B}^{+})$ ratio is a bit lower than the one between non-prompt Λ_{c}^{+} and D^{0} mesons, however it has to be considered that the normalization is slightly different. In the LHCb result the production cross sections of B^{0} and B^{+} mesons, i.e. the total yield of non-strange B mesons is used, while the non-prompt D^{0}, used in this ratio, accounts for about 70% of the non-strange D mesons. Also the fraction of B^{0} and B^{+} mesons decaying to Λ_{c}^{+} and $\mathrm{D}_{\mathrm{s}}^{+}$, as well as the Λ_{b}^{0} and $\mathrm{B}_{\mathrm{s}}^{0}$ hadrons decaying to D^{0} mesons influence the ratio. In addition, in the non-prompt $\Lambda_{\mathrm{c}}^{+}/\mathrm{D}^{0}$ ratio, the $\mathrm{h_b} \rightarrow \mathrm{h_c} + \mathrm{X}$ decay kinematics is expected to slightly modify the p_{T} dependence compared to the one of the ratio between beauty hadrons. Interestingly, all the measurements for beauty, charm, and strange hadrons show a similar trend as a function of p_{T} and are compatible within the uncertainties. The p/π^{+} production ratio also features a similar p_{T} dependence, however it is lower in absolute terms. The experimental values are compared with the corresponding predictions obtained with PYTHIA 8 simulations, using different tunes and the same rapidity ranges of the experimental results. In the top-left panel, the results obtained with the Monash 2013 tune [58], which implements a fragmentation process tuned to reproduce the measurements in $\mathrm{e}^{+}\mathrm{e}^{-}$ collisions, is reported. Here, all the baryon-to-meson ratios are underestimated by PYTHIA 8 except for the p/π^{+} ratio for which the model prediction is rather good at low p_{T}. A better agreement is instead obtained with the CLR-BLC tunes (i.e. Mode 0, 2, and 3), shown

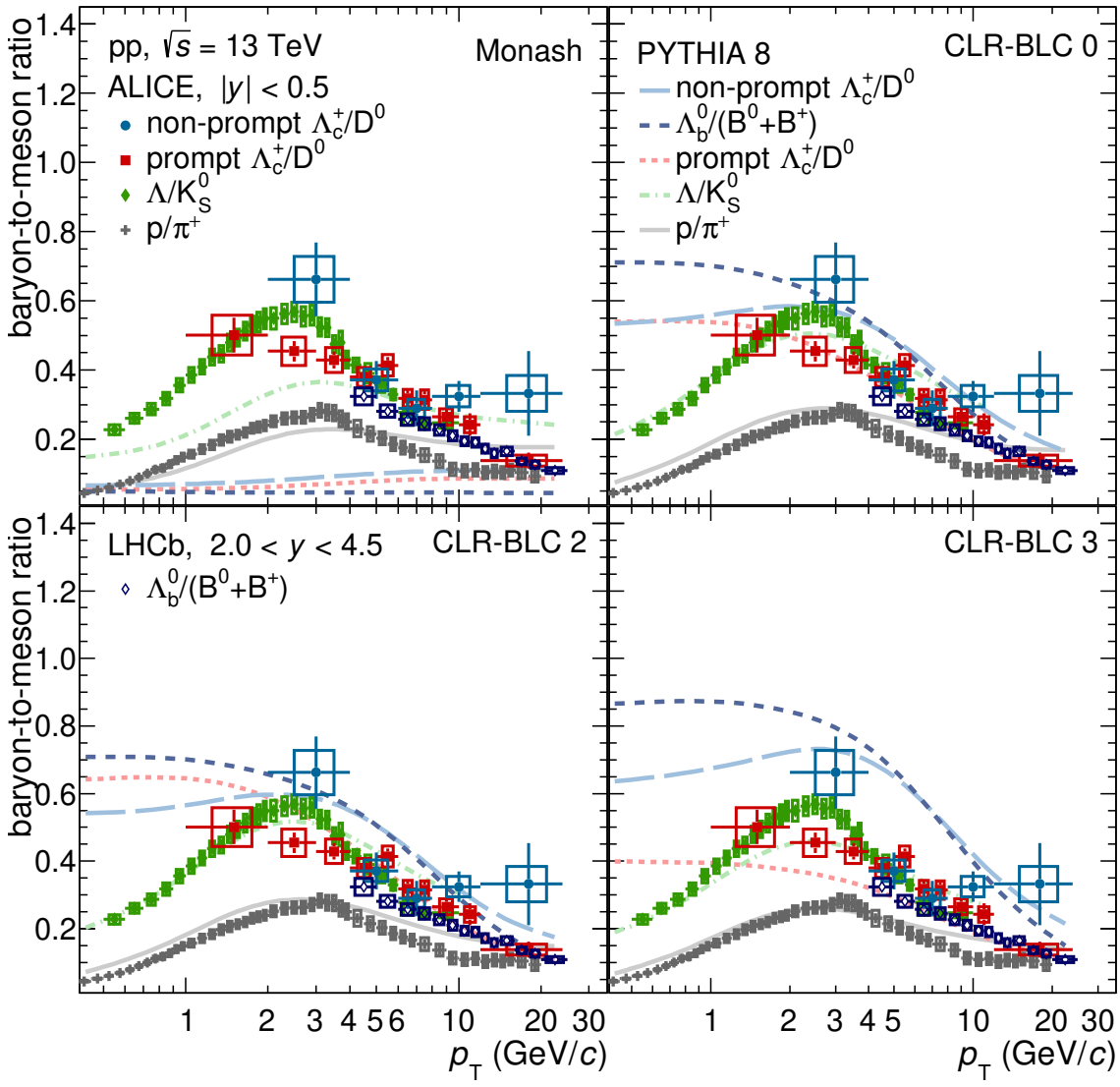

Figure 6: Non-prompt Λ_c^+/D^0, prompt Λ_c^+/D^0 [27], Λ/K_S^0 [67], and p/π^+ [67] ratios measured in pp collisions at $\sqrt{s} = 13$ TeV at midrapidity ($|y| < 0.5$) compared with the $\Lambda_b^0/(B^0 + B^+)$ ratio measured by the LHCb Collaboration at forward rapidity ($2.5 < y < 4$) [39] and with predictions obtained with the PYTHIA 8 MC generator with the Monash 2013 tune [50, 58] and the CLR-BLC modes 0, 2, and 3 [37] in the corresponding rapidity range with respect to data.

in the other three panels of Fig. 6. These three tunes are characterized by different constraints on the time dilation and causality, as defined in Ref. [37]. The time parameters are relevant in this model, because two strings can reconnect if they are able to resolve each other during the time between their formation and hadronization, taking also into account time-dilation effects caused by relative boosts. The Mode 0 and 2 settings, reported in the top-right and bottom-left panels of Fig. 6 respectively, predict a similar baryon-to-meson ratio for the strange, charm, and beauty flavors for $p_T > 2$ GeV/c and a significantly higher ratio for heavy-flavor hadrons than strange hadrons for lower p_T (e.g., a factor three is predicted at $p_T \approx 400$ MeV/c). Despite the agreement with the data is significantly improved compared to the Monash tune, the measurements of beauty hadrons are overestimated for $p_T \lesssim 10$ GeV/c. Instead, the Mode 3 (bottom-right panel of Fig. 6) underestimates the ratio for charm hadrons for $p_T \lesssim 12$ GeV/c and overestimates that of beauty hadrons in the same p_T interval, quantitatively more than the other two CLR-BLC modes. The features, observed in all comparisons with PYTHIA 8 tunes, indicate that more precise

Table 2: $p_{\rm T}$-integrated $\Lambda_{\rm c}^{+}/{\rm D}^{0}$ production ratio measured at midrapidity ($|y| < 0.5$) in pp collisions at $\sqrt{s} = 13$ TeV and in $\rm e^{+}e^{-}$ collisions at LEP [68] for prompt and non-prompt production.

	ALICE	LEP average [68]
prompt $\Lambda_{\rm c}^{+}/{\rm D}^{0}$	$0.49 \pm 0.02({\rm stat})^{+0.05}_{-0.04}({\rm syst})^{+0.01}_{-0.03}({\rm syst})$ [60]	0.105 ± 0.013
non-prompt $\Lambda_{\rm c}^{+}/{\rm D}^{0}$	$0.47 \pm 0.06({\rm stat}) \pm 0.04({\rm syst})^{+0.03}_{-0.04}({\rm extrap})$	0.124 ± 0.016

measurements of the baryon-to-meson ratios, especially those including beauty-hadron measurements at very low $p_{\rm T}$ ($p_{\rm T} < 2$ GeV/c) are crucial for tuning the model parameters involving the reconnection of quarks via junction topologies and to possibly validate this as the mechanism responsible of the baryon enhancement observed in hadron collisions compared to $\rm e^{+}e^{-}$ collisions. It is worth pointing out that other theoretical models are proposed to describe the enhancement, based on different hadronization mechanisms (e.g. recombination).

The $p_{\rm T}$-integrated non-prompt $\Lambda_{\rm c}^{+}/{\rm D}^{0}$ ratio was computed by dividing the $p_{\rm T}$-integrated cross sections reported in Table 1. All the systematic uncertainties, except for those related to the tracking efficiency, were propagated as uncorrelated in the ratio. The resulting value is compatible with the one measured for promptly produced particles and significantly higher than that measured in $\rm e^{+}e^{-}$ collisions at LEP [68]. All the values are reported in Table 2.

6 Conclusions

In summary, the $p_{\rm T}$-differential and $p_{\rm T}$-integrated production cross sections of non-prompt $\Lambda_{\rm c}^{+}$ and $\rm D^{0}$ hadrons were measured for the first time at midrapidity in pp collisions at $\sqrt{s} = 13$ TeV. The results are compatible with the theoretical models based on FONLL calculations with the $f(\rm b \to \Lambda_{b}^{0})$ and $f(\rm b \to B)$ fragmentation fractions measured by LHCb and at $\rm e^{+}e^{-}$, respectively, suggesting a similar beauty-baryon enhancement at forward and midrapidity in pp collisions. Furthermore, the results are in agreement with the TAMU statistical hadronization model for the relative abundances of different beauty hadron species. The extrapolated $\rm b\overline{b}$ production cross section at midrapidity per unit of rapidity is found to be compatible with pQCD calculations with FONLL and NNLO accuracy. The measured baryon-to-meson ratios of light flavor, strange, charm, and beauty hadrons show a similar $p_{\rm T}$ trend. In addition, all ratios, except the $\rm p/\pi^{+}$, are significantly higher than the values measured in $\rm e^{+}e^{-}$ collisions. The $p_{\rm T}$-differential baryon-to-meson ratios have been compared to predictions of the TAMU statistical hadronization model and to the PYTHIA 8 simulations, that include the color-reconnection mechanism in the string fragmentation and indicate that all the flavors have to be considered simultaneously in order to obtain the best tuning of the model parameters involving the reconnection of quarks via junction topologies. This feature asks for more precise results, including a direct measurement of beauty hadrons especially in the same $p_{\rm T}$ and rapidity range and the $p_{\rm T} < 4$ GeV/c region, which can be reached with the data collected in the LHC Run 3 data taking period.

Acknowledgements

The ALICE Collaboration would like to thank all its engineers and technicians for their invaluable contributions to the construction of the experiment and the CERN accelerator teams for the outstanding performance of the LHC complex. The ALICE Collaboration gratefully acknowledges the resources and support provided by all Grid centres and the Worldwide LHC Computing Grid (WLCG) collaboration. The ALICE Collaboration acknowledges the following funding agencies for their support in building and running the ALICE detector: A. I. Alikhanyan National Science Laboratory (Yerevan Physics Institute) Foundation (ANSL), State Committee of Science and World Federation of Scientists (WFS),

Armenia; Austrian Academy of Sciences, Austrian Science Fund (FWF): [M 2467-N36] and Nationalstiftung für Forschung, Technologie und Entwicklung, Austria; Ministry of Communications and High Technologies, National Nuclear Research Center, Azerbaijan; Conselho Nacional de Desenvolvimento Científico e Tecnológico (CNPq), Financiadora de Estudos e Projetos (Finep), Fundação de Amparo à Pesquisa do Estado de São Paulo (FAPESP) and Universidade Federal do Rio Grande do Sul (UFRGS), Brazil; Bulgarian Ministry of Education and Science, within the National Roadmap for Research Infrastructures 2020-2027 (object CERN), Bulgaria; Ministry of Education of China (MOEC) , Ministry of Science & Technology of China (MSTC) and National Natural Science Foundation of China (NSFC), China; Ministry of Science and Education and Croatian Science Foundation, Croatia; Centro de Aplicaciones Tecnológicas y Desarrollo Nuclear (CEADEN), Cubaenergía, Cuba; Ministry of Education, Youth and Sports of the Czech Republic, Czech Republic; The Danish Council for Independent Research | Natural Sciences, the VILLUM FONDEN and Danish National Research Foundation (DNRF), Denmark; Helsinki Institute of Physics (HIP), Finland; Commissariat à l'Energie Atomique (CEA) and Institut National de Physique Nucléaire et de Physique des Particules (IN2P3) and Centre National de la Recherche Scientifique (CNRS), France; Bundesministerium für Bildung und Forschung (BMBF) and GSI Helmholtzzentrum für Schwerionenforschung GmbH, Germany; General Secretariat for Research and Technology, Ministry of Education, Research and Religions, Greece; National Research, Development and Innovation Office, Hungary; Department of Atomic Energy Government of India (DAE), Department of Science and Technology, Government of India (DST), University Grants Commission, Government of India (UGC) and Council of Scientific and Industrial Research (CSIR), India; National Research and Innovation Agency - BRIN, Indonesia; Istituto Nazionale di Fisica Nucleare (INFN), Italy; Japanese Ministry of Education, Culture, Sports, Science and Technology (MEXT) and Japan Society for the Promotion of Science (JSPS) KAKENHI, Japan; Consejo Nacional de Ciencia (CONACYT) y Tecnología, through Fondo de Cooperación Internacional en Ciencia y Tecnología (FONCICYT) and Dirección General de Asuntos del Personal Academico (DGAPA), Mexico; Nederlandse Organisatie voor Wetenschappelijk Onderzoek (NWO), Netherlands; The Research Council of Norway, Norway; Commission on Science and Technology for Sustainable Development in the South (COMSATS), Pakistan; Pontificia Universidad Católica del Perú, Peru; Ministry of Education and Science, National Science Centre and WUT ID-UB, Poland; Korea Institute of Science and Technology Information and National Research Foundation of Korea (NRF), Republic of Korea; Ministry of Education and Scientific Research, Institute of Atomic Physics, Ministry of Research and Innovation and Institute of Atomic Physics and Universitatea Nationala de Stiinta si Tehnologie Politehnica Bucuresti, Romania; Ministry of Education, Science, Research and Sport of the Slovak Republic, Slovakia; National Research Foundation of South Africa, South Africa; Swedish Research Council (VR) and Knut & Alice Wallenberg Foundation (KAW), Sweden; European Organization for Nuclear Research, Switzerland; Suranaree University of Technology (SUT), National Science and Technology Development Agency (NSTDA) and National Science, Research and Innovation Fund (NSRF via PMU-B B05F650021), Thailand; Turkish Energy, Nuclear and Mineral Research Agency (TENMAK), Turkey; National Academy of Sciences of Ukraine, Ukraine; Science and Technology Facilities Council (STFC), United Kingdom; National Science Foundation of the United States of America (NSF) and United States Department of Energy, Office of Nuclear Physics (DOE NP), United States of America. In addition, individual groups or members have received support from: European Research Council, Strong 2020 - Horizon 2020 (grant nos. 950692, 824093), European Union; Academy of Finland (Center of Excellence in Quark Matter) (grant nos. 346327, 346328), Finland.

References

[1] **ALICE** Collaboration, S. Acharya *et al.*, "Measurement of D^0 , D^+ , D^{*+} and D_s^+ production in pp collisions at $\sqrt{s} = 5.02$ TeV with ALICE", *Eur. Phys. J. C* **79** (2019) 388, arXiv:1901.07979 [nucl-ex].

[2] **ALICE** Collaboration, S. Acharya *et al.*, "Measurement of beauty and charm production in pp collisions at $\sqrt{s}$ = 5.02 TeV via non-prompt and prompt D mesons", *JHEP* **05** (2021) 220, arXiv:2102.13601 [nucl-ex].

[3] **ALICE** Collaboration, S. Acharya *et al.*, "Prompt and non-prompt J/ψ production cross sections at midrapidity in proton-proton collisions at $\sqrt{s}$ = 5.02 and 13 TeV", *JHEP* **03** (2022) 190, arXiv:2108.02523 [nucl-ex].

[4] **ALICE** Collaboration, S. Acharya *et al.*, "Measurement of electrons from semileptonic heavy-flavour hadron decays at midrapidity in pp and Pb–Pb collisions at $\sqrt{s_{\rm NN}}$ = 5.02 TeV", *Phys. Lett. B* **804** (2020) 135377, arXiv:1910.09110 [nucl-ex].

[5] **CMS** Collaboration, V. Khachatryan *et al.*, "Measurement of the total and differential inclusive B^+ hadron cross sections in pp collisions at $\sqrt{s}$ = 13 TeV", *Phys. Lett. B* **771** (2017) 435–456, arXiv:1609.00873 [hep-ex].

[6] **CMS** Collaboration, A. M. Sirunyan *et al.*, "Nuclear modification factor of $\rm D^0$ mesons in PbPb collisions at $\sqrt{s_{\rm NN}} = 5.02$ TeV", *Phys. Lett. B* **782** (2018) 474–496, arXiv:1708.04962 [nucl-ex].

[7] **CMS** Collaboration, A. M. Sirunyan *et al.*, "Studies of Beauty Suppression via Nonprompt D^0 Mesons in Pb-Pb Collisions at $Q^2 = 4$ GeV^2", *Phys. Rev. Lett.* **123** (2019) 022001, arXiv:1810.11102 [hep-ex].

[8] **LHCb** Collaboration, R. Aaij *et al.*, "Measurements of prompt charm production cross-sections in pp collisions at $\sqrt{s} = 13$ TeV", *JHEP* **03** (2016) 159, arXiv:1510.01707 [hep-ex]. [Erratum: *JHEP* **09** (2016) 013, Erratum: *JHEP* **05** (2017) 074].

[9] **LHCb** Collaboration, R. Aaij *et al.*, "Measurements of prompt charm production cross-sections in pp collisions at $\sqrt{s} = 5$ TeV", *JHEP* **06** (2017) 147, arXiv:1610.02230 [hep-ex].

[10] **LHCb** Collaboration, R. Aaij *et al.*, "Measurement of the $B^\pm$ production cross-section in pp collisions at $\sqrt{s} = 7$ and 13 TeV", *JHEP* **12** (2017) 026, arXiv:1710.04921 [hep-ex].

[11] **ATLAS** Collaboration, G. Aad *et al.*, "Measurement of $D^{*\pm}$, $D^\pm$ and $D_s^\pm$ meson production cross sections in pp collisions at $\sqrt{s} = 7$ TeV with the ATLAS detector", *Nucl. Phys. B* **907** (2016) 717–763, arXiv:1512.02913 [hep-ex].

[12] **ALICE** Collaboration, "The ALICE experiment – A journey through QCD", arXiv:2211.04384 [nucl-ex].

[13] M. Cacciari, M. Greco, and P. Nason, "The $p_{\rm T}$ spectrum in heavy flavor hadroproduction", *JHEP* **05** (1998) 007, arXiv:hep-ph/9803400.

[14] M. Cacciari, S. Frixione, and P. Nason, "The $p_{\rm T}$ spectrum in heavy flavor photoproduction", *JHEP* **03** (2001) 006, arXiv:hep-ph/0102134.

[15] M. Cacciari, S. Frixione, N. Houdeau, M. L. Mangano, P. Nason, and G. Ridolfi, "Theoretical predictions for charm and bottom production at the LHC", *JHEP* **10** (2012) 137, arXiv:1205.6344 [hep-ph].

[16] B. Kniehl, G. Kramer, I. Schienbein, and H. Spiesberger, "Inclusive $D^{*\pm}$ production in $p\overline{p}$ collisions with massive charm quarks", *Phys. Rev. D* **71** (2005) 014018, arXiv:hep-ph/0410289.

[17] B. Kniehl, G. Kramer, I. Schienbein, and H. Spiesberger, "Inclusive Charmed-Meson Production at the CERN LHC", *Eur. Phys. J. C* **72** (2012) 2082, arXiv:1202.0439 [hep-ph].

[18] M. Benzke, M. Garzelli, B. Kniehl, G. Kramer, S. Moch, and G. Sigl, "Prompt neutrinos from atmospheric charm in the general-mass variable-flavor-number scheme", *JHEP* **12** (2017) 021, arXiv:1705.10386 [hep-ph].

[19] G. Kramer and H. Spiesberger, "Study of heavy meson production in p–Pb collisions at $\sqrt{s}$= 5.02 TeV in the general-mass variable-flavour-number scheme", *Nucl. Phys. B* **925** (2017) 415–430, arXiv:1703.04754 [hep-ph].

[20] I. Helenius and H. Paukkunen, "Revisiting the D-meson hadroproduction in general-mass variable flavour number scheme", *JHEP* **05** (2018) 196, arXiv:1804.03557 [hep-ph].

[21] P. Bolzoni and G. Kramer, "Inclusive charmed-meson production from bottom hadron decays at the LHC", *J. Phys. G* **41** (2014) 075006, arXiv:1310.2924 [hep-ph].

[22] S. Catani, S. Devoto, M. Grazzini, S. Kallweit, and J. Mazzitelli, "Bottom-quark production at hadron colliders: fully differential predictions in NNLO QCD", *JHEP* **03** (2021) 029, arXiv:2010.11906 [hep-ph].

[23] E. Braaten, K.-m. Cheung, S. Fleming, and T. C. Yuan, "Perturbative QCD fragmentation functions as a model for heavy quark fragmentation", *Phys. Rev. D* **51** (1995) 4819–4829, arXiv:hep-ph/9409316.

[24] **ALICE** Collaboration, S. Acharya *et al.*, "Measurement of the cross sections of Ξ_c^0 and Ξ_c^+ baryons and of the branching-fraction ratio BR($\Xi_c^0 \to \Xi^- e^+ \nu_e$)/BR($\Xi_c^0 \to \Xi^- \pi^+$) in pp collisions at 13 TeV", *Phys. Rev. Lett.* **127** (2021) 272001, arXiv:2105.05187 [nucl-ex].

[25] **ALICE** Collaboration, S. Acharya *et al.*, "Λ_c^+ production and baryon-to-meson ratios in pp and p–Pb collisions at $\sqrt{s_{NN}}$=5.02 TeV at the LHC", *Phys. Rev. Lett.* **127** (2021) 202301, arXiv:2011.06078 [nucl-ex].

[26] **ALICE** Collaboration, S. Acharya *et al.*, "Λ_c^+ production in pp and in p–Pb collisions at $\sqrt{s_{NN}}$=5.02 TeV", *Phys. Rev. C* **104** (2021) 054905, arXiv:2011.06079 [nucl-ex].

[27] **ALICE** Collaboration, S. Acharya *et al.*, "Measurement of Prompt D^0, Λ_c^+, and $\Sigma_c^{0,++}$(2455) production in proton–proton collisions at $\sqrt{s}$ = 13 TeV", *Phys. Rev. Lett.* **128** (2022) 012001, arXiv:2106.08278 [hep-ex].

[28] **ALICE** Collaboration, S. Acharya *et al.*, "First measurement of Ωc0 production in pp collisions at s=13 TeV", *Phys. Lett. B* **846** (2023) 137625, arXiv:2205.13993 [nucl-ex].

[29] **CMS** Collaboration, A. M. Sirunyan *et al.*, "Production of Λ_c^+ baryons in proton-proton and lead-lead collisions at $\sqrt{s_{NN}} = 5.02$ TeV", *Phys. Lett. B* **803** (2020) 135328, arXiv:1906.03322 [hep-ex].

[30] **ALICE** Collaboration, S. Acharya *et al.*, "Charm-quark fragmentation fractions and production cross section at midrapidity in pp collisions at the LHC", *Phys. Rev. D* **105** (2022) L011103, arXiv:2105.06335 [nucl-ex].

[31] **ALICE** Collaboration, S. Acharya *et al.*, "First measurement of Λc+ production down to pT=0 in pp and p-Pb collisions at sNN=5.02 TeV", *Phys. Rev. C* **107** (2023) 064901, arXiv:2211.14032 [nucl-ex].

[32] **ALICE** Collaboration, S. Acharya *et al.*, "Measurement of the production cross section of prompt Ξ_c^0 baryons at midrapidity in pp collisions at $\sqrt{s}$ = 5.02 TeV", *JHEP* **10** (2021) 159, arXiv:2105.05616 [nucl-ex].

[33] J. Song, H.-H. Li, and F.-L. Shao, "New feature of low p_T charm quark hadronization in pp collisions at $\sqrt{s} = 7$ TeV", *Eur. Phys. J. C* **78** (2018) 344, arXiv:1801.09402 [hep-ph].

[34] V. Minissale, S. Plumari, and V. Greco, "Charm hadrons in pp collisions at LHC energy within a coalescence plus fragmentation approach", *Phys. Lett. B* **821** (2021) 136622, arXiv:2012.12001 [hep-ph].

[35] D. Ebert, R. N. Faustov, and V. O. Galkin, "Spectroscopy and Regge trajectories of heavy baryons in the relativistic quark-diquark picture", *Phys. Rev. D* **84** (2011) 014025, arXiv:1105.0583 [hep-ph].

[36] M. He and R. Rapp, "Charm-Baryon Production in Proton-Proton Collisions", *Phys. Lett. B* **795** (2019) 117–121, arXiv:1902.08889 [nucl-th].

[37] J. R. Christiansen and P. Z. Skands, "String Formation Beyond Leading Colour", *JHEP* **08** (2015) 003, arXiv:1505.01681 [hep-ph].

[38] **LHCb** Collaboration, R. Aaij *et al.*, "Study of the production of Λ_b^0 and $\overline{B}^0$ hadrons in pp collisions and first measurement of the $\Lambda_b^0 \to J/\psi p K^-$ branching fraction", *Chin. Phys. C* **40** (2016) 011001, arXiv:1509.00292 [hep-ex].

[39] **LHCb** Collaboration, R. Aaij *et al.*, "Measurement of b hadron fractions in 13 TeV pp collisions", *Phys. Rev. D* **100** (2019) 031102, arXiv:1902.06794 [hep-ex].

[40] **LHCb** Collaboration, R. Aaij *et al.*, "Prompt charm production in pp collisions at $\sqrt{s}$ =7 TeV", *Nucl. Phys. B* **871** (2013) 1–20, arXiv:1302.2864 [hep-ex].

[41] **LHCb** Collaboration, R. Aaij *et al.*, "Prompt Λ_c^+ production in pPb collisions at $\sqrt{s_{NN}} = 5.02$ TeV", *JHEP* **02** (2019) 102, arXiv:1809.01404 [hep-ex].

[42] **CMS** Collaboration, A. M. Sirunyan *et al.*, "Measurement of the $B^{\pm}$ Meson Nuclear Modification Factor in Pb-Pb Collisions at $\sqrt{s_{NN}} = 5.02$ TeV", *Phys. Rev. Lett.* **119** (2017) 152301, arXiv:1705.04727 [hep-ex].

[43] **CMS** Collaboration, A. M. Sirunyan *et al.*, "Measurement of $\mathrm{B_s^0}$ meson production in pp and PbPb collisions at $\sqrt{s_{\mathrm{NN}}} = 5.02$ TeV", *Phys. Lett. B* **796** (2019) 168–190, arXiv:1810.03022 [hep-ex].

[44] **ATLAS** Collaboration, G. Aad *et al.*, "Measurement of the differential cross-section of B^+ meson production in pp collisions at $\sqrt{s}$ = 7 TeV at ATLAS", *JHEP* **10** (2013) 042, arXiv:1307.0126 [hep-ex].

[45] **CMS** Collaboration, V. Khachatryan *et al.*, "Measurement of the B^+ Production Cross Section in pp Collisions at $\sqrt{s} = 7$ TeV", *Phys. Rev. Lett.* **106** (2011) 112001, arXiv:1101.0131 [hep-ex].

[46] **CMS** Collaboration, S. Chatrchyan *et al.*, "Measurement of the Strange B Meson Production Cross Section with J/Psi ϕ Decays in pp Collisions at $\sqrt{s} = 7$ TeV", *Phys. Rev. D* **84** (2011) 052008, arXiv:1106.4048 [hep-ex].

[47] **CMS** Collaboration, S. Chatrchyan *et al.*, "Measurement of the B^0 production cross section in pp Collisions at $\sqrt{s} = 7$ TeV", *Phys. Rev. Lett.* **106** (2011) 252001, arXiv:1104.2892 [hep-ex].

[48] **CMS** Collaboration, S. Chatrchyan *et al.*, "Measurement of the Λ_b cross section and the $\bar{\Lambda}_b$ to Λ_b ratio with $J/\Psi\Lambda$ decays in pp collisions at $\sqrt{s} = 7$ TeV", *Phys. Lett. B* **714** (2012) 136–157, arXiv:1205.0594 [hep-ex].

[49] M. He and R. Rapp, "Bottom hadro-chemistry in high-energy hadronic collisions", *Phys. Rev. Lett.* **131** (2023) 012301, arXiv:2209.13419 [hep-ph].

[50] T. Sjöstrand, S. Ask, J. R. Christiansen, R. Corke, N. Desai, P. Ilten, S. Mrenna, S. Prestel, C. O. Rasmussen, and P. Z. Skands, "An Introduction to PYTHIA 8.2", *Comput. Phys. Commun.* **191** (2015) 159–177, arXiv:1410.3012 [hep-ph].

[51] **ALICE** Collaboration, B. Abelev *et al.*, "Performance of the ALICE Experiment at the CERN LHC", *Int. J. Mod. Phys. A* **29** (2014) 1430044, arXiv:1402.4476 [nucl-ex].

[52] **ALICE** Collaboration, K. Aamodt *et al.*, "The ALICE experiment at the CERN LHC", *JINST* **3** (2008) S08002.

[53] **ALICE** Collaboration, S. Acharya *et al.*, "ALICE 2016-2017-2018 luminosity determination for pp collisions at $\sqrt{s} = 13$ TeV", *ALICE-PUBLIC-2021-005* (2021) . https://cds.cern.ch/record/2776672/.

[54] **Particle Data Group** Collaboration, R. L. Workman and Others, "Review of Particle Physics", *PTEP* **2022** (2022) 083C01.

[55] I. Kisel, I. Kulakov, and M. Zyzak, "Standalone First Level Event Selection Package for the CBM Experiment", *IEEE Transactions on Nuclear Science* **60** (2013) 3703–3708.

[56] T. Chen and C. Guestrin, "Xgboost: A scalable tree boosting system", in *Proceedings of the 22nd ACM SIGKDD International Conference on Knowledge Discovery and Data Mining*, pp. 785–794. 2016. arXiv:1603.02754 [cs.LG].

[57] L. Barioglio, F. Catalano, M. Concas, P. Fecchio, F. Grosa, F. Mazzaschi, and M. Puccio, "hipe4ml/hipe4ml", July, 2021. https://doi.org/10.5281/zenodo.5070132.

[58] P. Skands, S. Carrazza, and J. Rojo, "Tuning PYTHIA 8.1: the Monash 2013 Tune", *Eur. Phys. J. C* **74** (2014) 3024, arXiv:1404.5630 [hep-ph].

[59] R. Brun, F. Carminati, and S. Giani, "CERN Program Library Long Write-up, W5013 GEANT Detector Description and Simulation Tool", Tech. Rep. CERN-W-5013, 1994. https://cds.cern.ch/record/2776672/.

[60] **ALICE** Collaboration, S. Acharya *et al.*, "Observation of a multiplicity dependence in the p_{T}-differential charm baryon-to-meson ratios in proton-proton collisions at $\sqrt{s} = 13$ TeV", *Phys. Lett. B* **829** (2022) 137065, arXiv:2111.11948 [nucl-ex].

[61] **Particle Data Group** Collaboration, R. L. Workman *et al.*, "Review of Particle Physics", *PTEP* **2022** (2022) 083C01.

[62] S. Alioli, P. Nason, C. Oleari, and E. Re, "A general framework for implementing NLO calculations in shower Monte Carlo programs: the POWHEG BOX", *JHEP* **06** (2010) 043, arXiv:1002.2581 [hep-ph].

[63] H.-L. Lai, M. Guzzi, J. Huston, Z. Li, P. M. Nadolsky, J. Pumplin, and C. P. Yuan, "New parton distributions for collider physics", *Phys. Rev. D* **82** (2010) 074024, arXiv:1007.2241 [hep-ph].

[64] S. Dulat, T.-J. Hou, J. Gao, M. Guzzi, J. Huston, P. Nadolsky, J. Pumplin, C. Schmidt, D. Stump, and C. P. Yuan, "New parton distribution functions from a global analysis of quantum chromodynamics", *Phys. Rev. D* **93** (2016) 033006, arXiv:1506.07443 [hep-ph].

[65] **ALICE** Collaboration, S. Acharya *et al.*, "Dielectron and heavy-quark production in inelastic and high-multiplicity proton–proton collisions at $\sqrt{s} = 13$ TeV", *Phys. Lett. B* **788** (2019) 505–518, arXiv:1805.04407 [hep-ex].

[66] **ALICE** Collaboration, S. Acharya *et al.*, "Dielectron production in proton-proton and proton-lead collisions at $\sqrt{s_{\rm NN}} = 5.02$ TeV", *Phys. Rev. C* **102** (2020) 055204, arXiv:2005.11995 [nucl-ex].

[67] **ALICE** Collaboration, S. Acharya *et al.*, "Production of light-flavor hadrons in pp collisions at $\sqrt{s} = 7$ and $\sqrt{s} = 13$ TeV", *Eur. Phys. J. C* **81** (2021) 256, arXiv:2005.11120 [nucl-ex].

[68] L. Gladilin, "Fragmentation fractions of c and b quarks into charmed hadrons at LEP", *Eur. Phys. J. C* **75** (2015) 19, arXiv:1404.3888 [hep-ex].

A The ALICE Collaboration

S. Acharya [128], D. Adamová [87], G. Aglieri Rinella [33], M. Agnello [30], N. Agrawal [52], Z. Ahammed [136], S. Ahmad [16], S.U. Ahn [72], I. Ahuja [38], A. Akindinov [142], M. Al-Turany [98], D. Aleksandrov [142], B. Alessandro [57], H.M. Alfanda [6], R. Alfaro Molina [68], B. Ali [16], A. Alici [26], N. Alizadehvandchali [117], A. Alkin [33], J. Alme [21], G. Alocco [53], T. Alt [65], A.R. Altamura [51], I. Altsybeev [96], M.N. Anaam [6], C. Andrei [46], N. Andreou [116], A. Andronic [127], V. Anguelov [95], F. Antinori [55], P. Antonioli [52], N. Apadula [75], L. Aphecetche [104], H. Appelshäuser [65], C. Arata [74], S. Arcelli [26], M. Aresti [23], R. Arnaldi [57], J.G.M.C.A. Arneiro [111], I.C. Arsene [20], M. Arslandok [139], A. Augustinus [33], R. Averbeck [98], M.D. Azmi [16], H. Baba[125], A. Badalà [54], J. Bae [105], Y.W. Baek [41], X. Bai [121], R. Bailhache [65], Y. Bailung [49], A. Balbino [30], A. Baldisseri [131], B. Balis [2], D. Banerjee [4], Z. Banoo [92], R. Barbera [27], F. Barile [32], L. Barioglio [96], M. Barlou[79], B. Barman[42], G.G. Barnaföldi [47], L.S. Barnby [86], V. Barret [128], L. Barreto [111], C. Bartels [120], K. Barth [33], E. Bartsch [65], N. Bastid [128], S. Basu [76], G. Batigne [104], D. Battistini [96], B. Batyunya [143], D. Bauri[48], J.L. Bazo Alba [102], I.G. Bearden [84], C. Beattie [139], P. Becht [98], D. Behera [49], I. Belikov [130], A.D.C. Bell Hechavarria [127], F. Bellini [26], R. Bellwied [117], S. Belokurova [142], G. Bencedi [47], S. Beole [25], Y. Berdnikov [142], A. Berdnikova [95], L. Bergmann [95], M.G. Besoiu [64], L. Betev [33], P.P. Bhaduri [136], A. Bhasin [92], M.A. Bhat [4], B. Bhattacharjee [42], L. Bianchi [25], N. Bianchi [50], J. Bielčík [36], J. Bielčíková [87], J. Biernat [108], A.P. Bigot [130], A. Bilandzic [96], G. Biro [47], S. Biswas [4], N. Bize [104], J.T. Blair [109], D. Blau [142], M.B. Blidaru [98], N. Bluhme[39], C. Blume [65], G. Boca [22,56], F. Bock [88], T. Bodova [21], A. Bogdanov[142], S. Boi [23], J. Bok [59], L. Boldizsár [47], M. Bombara [38], P.M. Bond [33], G. Bonomi [135,56], H. Borel [131], A. Borissov [142], A.G. Borquez Carcamo [95], H. Bossi [139], E. Botta [25], Y.E.M. Bouziani [65], L. Bratrud [65], P. Braun-Munzinger [98], M. Bregant [111], M. Broz [36], G.E. Bruno [97,32], M.D. Buckland [24], D. Budnikov [142], H. Buesching [65], S. Bufalino [30], P. Buhler [103], N. Burmasov [142], Z. Buthelezi [69,124], A. Bylinkin [21], S.A. Bysiak[108], M. Cai [6], H. Caines [139], A. Caliva [29], E. Calvo Villar [102], J.M.M. Camacho [110], P. Camerini [24], F.D.M. Canedo [111], M. Carabas [114], A.A. Carballo [33], F. Carnesecchi [33], R. Caron [129], L.A.D. Carvalho [111], J. Castillo Castellanos [131], F. Catalano [33,25], C. Ceballos Sanchez [143], I. Chakaberia [75], P. Chakraborty [48], S. Chandra [136], S. Chapeland [33], M. Chartier [120], S. Chattopadhyay [136], S. Chattopadhyay [100], T.G. Chavez [45], T. Cheng [98,6], C. Cheshkov [129], B. Cheynis [129], V. Chibante Barroso [33], D.D. Chinellato [112], E.S. Chizzali[II,96], J. Cho [59], S. Cho [59], P. Chochula [33], D. Choudhury[42], P. Christakoglou [85], C.H. Christensen [84], P. Christiansen [76], T. Chujo [126], M. Ciacco [30], C. Cicalo [53], F. Cindolo [52], M.R. Ciupek[98], G. Clai[III,52], F. Colamaria [51], J.S. Colburn[101], D. Colella [97,32], M. Colocci [26], M. Concas [IV,57], G. Conesa Balbastre [74], Z. Conesa del Valle [132], G. Contin [24], J.G. Contreras [36], M.L. Coquet [131], P. Cortese [134,57], M.R. Cosentino [113], F. Costa [33], S. Costanza [22,56], C. Cot [132], J. Crkovská [95], P. Crochet [128], R. Cruz-Torres [75], P. Cui [6], A. Dainese [55], M.C. Danisch [95], A. Danu [64], P. Das [81], P. Das [4], S. Das [4], A.R. Dash [127], S. Dash [48], R.M.H. David[45], A. De Caro [29], G. de Cataldo [51], J. de Cuveland[39], A. De Falco [23], D. De Gruttola [29], N. De Marco [57], C. De Martin [24], S. De Pasquale [29], R. Deb [135], R. Del Grande [96], L. Dello Stritto [29], W. Deng [6], P. Dhankher [19], D. Di Bari [32], A. Di Mauro [33], B. Diab [131], R.A. Diaz [143,7], T. Dietel [115], Y. Ding [6], R. Divià [33], D.U. Dixit [19], Ø. Djuvsland[21], U. Dmitrieva [142], A. Dobrin [64], B. Dönigus [65], J.M. Dubinski [137], A. Dubla [98], S. Dudi [91], P. Dupieux [128], M. Durkac[107], N. Dzalaiova[13], T.M. Eder [127], R.J. Ehlers [75], F. Eisenhut [65], R. Ejima[93], D. Elia [51], B. Erazmus [104], F. Ercolessi [26], F. Erhardt [90], M.R. Ersdal[21], B. Espagnon [132], G. Eulisse [33], D. Evans [101], S. Evdokimov [142], L. Fabbietti [96], M. Faggin [28], J. Faivre [74], F. Fan [6], W. Fan [75], A. Fantoni [50], M. Fasel [88], P. Fecchio[30], A. Feliciello [57], G. Feofilov [142], A. Fernández Téllez [45], L. Ferrandi [111], M.B. Ferrer [33], A. Ferrero [131], C. Ferrero [57], A. Ferretti [25], V.J.G. Feuillard [95], V. Filova [36], D. Finogeev [142], F.M. Fionda [53], F. Flor [117], A.N. Flores [109], S. Foertsch [69], I. Fokin [95], S. Fokin [142], E. Fragiacomo [58], E. Frajna [47], U. Fuchs [33], N. Funicello [29], C. Furget [74], A. Furs [142], T. Fusayasu [99], J.J. Gaardhøje [84], M. Gagliardi [25], A.M. Gago [102], T. Gahlaut[48], C.D. Galvan [110], D.R. Gangadharan [117], P. Ganoti [79], C. Garabatos [98], A.T. Garcia [132], J.R.A. Garcia [45], E. Garcia-Solis [9], C. Gargiulo [33], K. Garner[127], P. Gasik [98], A. Gautam [119], M.B. Gay Ducati [67], M. Germain [104], A. Ghimouz[126], C. Ghosh[136], M. Giacalone [52], G. Gioachin [30], P. Giubellino [98,57], P. Giubilato [28], A.M.C. Glaenzer [131], P. Glässel [95], E. Glimos [123], D.J.Q. Goh[77], V. Gonzalez [138], M. Gorgon [2], K. Goswami [49], S. Gotovac[34], V. Grabski [68], L.K. Graczykowski [137], E. Grecka [87], A. Grelli [60], C. Grigoras [33], V. Grigoriev [142], S. Grigoryan [143,1], F. Grosa [33], J.F. Grosse-Oetringhaus [33], R. Grosso [98], D. Grund [36], G.G. Guardiano [112], R. Guernane [74], M. Guilbaud [104], K. Gulbrandsen [84], T. Gündem [65], T. Gunji [125], W. Guo [6], A. Gupta [92], R. Gupta [92],

R. Gupta [49], S.P. Guzman [45], K. Gwizdziel [137], L. Gyulai [47], C. Hadjidakis [132], F.U. Haider [92], H. Hamagaki [77], A. Hamdi [75], Y. Han [140], B.G. Hanley [138], R. Hannigan [109], J. Hansen [76], M.R. Haque [137], J.W. Harris [139], A. Harton [9], H. Hassan [88], D. Hatzifotiadou [52], P. Hauer [43], L.B. Havener [139], S.T. Heckel [96], E. Hellbär [98], H. Helstrup [35], M. Hemmer [65], T. Herman [36], G. Herrera Corral [8], F. Herrmann[127], S. Herrmann [129], K.F. Hetland [35], B. Heybeck [65], H. Hillemanns [33], B. Hippolyte [130], F.W. Hoffmann [71], B. Hofman [60], G.H. Hong [140], M. Horst [96], A. Horzyk [2], Y. Hou [6], P. Hristov [33], C. Hughes [123], P. Huhn[65], L.M. Huhta [118], T.J. Humanic [89], A. Hutson [117], D. Hutter [39], R. Ilkaev[142], H. Ilyas [14], M. Inaba [126], G.M. Innocenti [33], M. Ippolitov [142], A. Isakov [85,87], T. Isidori [119], M.S. Islam [100], M. Ivanov[13], M. Ivanov [98], V. Ivanov [142], K.E. Iversen [76], M. Jablonski [2], B. Jacak [75], N. Jacazio [26], P.M. Jacobs [75], S. Jadlovska[107], J. Jadlovsky[107], S. Jaelani [83], C. Jahnke [112], M.J. Jakubowska [137], M.A. Janik [137], T. Janson[71], S. Ji [17], S. Jia [10], A.A.P. Jimenez [66], F. Jonas [88], D.M. Jones [120], J.M. Jowett [33,98], J. Jung [65], M. Jung [65], A. Junique [33], A. Jusko [101], M.J. Kabus [33,137], J. Kaewjai[106], P. Kalinak [61], A.S. Kalteyer [98], A. Kalweit [33], V. Kaplin [142], A. Karasu Uysal [73], D. Karatovic [90], O. Karavichev [142], T. Karavicheva [142], P. Karczmarczyk [137], E. Karpechev [142], U. Kebschull [71], R. Keidel [141], D.L.D. Keijdener[60], M. Keil [33], B. Ketzer [43], S.S. Khade [49], A.M. Khan [121,6], S. Khan [16], A. Khanzadeev [142], Y. Kharlov [142], A. Khatun [119], A. Khuntia [36], B. Kileng [35], B. Kim [105], C. Kim [17], D.J. Kim [118], E.J. Kim [70], J. Kim [140], J.S. Kim [41], J. Kim [59], J. Kim [70], M. Kim [19], S. Kim [18], T. Kim [140], K. Kimura [93], S. Kirsch [65], I. Kisel [39], S. Kiselev [142], A. Kisiel [137], J.P. Kitowski [2], J.L. Klay [5], J. Klein [33], S. Klein [75], C. Klein-Bösing [127], M. Kleiner [65], T. Klemenz [96], A. Kluge [33], A.G. Knospe [117], C. Kobdaj [106], T. Kollegger[98], A. Kondratyev [143], N. Kondratyeva [142], E. Kondratyuk [142], J. Konig [65], S.A. Konigstorfer [96], P.J. Konopka [33], G. Kornakov [137], M. Korwieser [96], S.D. Koryciak [2], A. Kotliarov [87], V. Kovalenko [142], M. Kowalski [108], V. Kozhuharov [37], I. Králik [61], A. Kravčáková [38], L. Krcal [33,39], M. Krivda [101,61], F. Krizek [87], K. Krizkova Gajdosova [33], M. Kroesen [95], M. Krüger [65], D.M. Krupova [36], E. Kryshen [142], V. Kučera [59], C. Kuhn [130], P.G. Kuijer [85], T. Kumaoka[126], D. Kumar[136], L. Kumar [91], N. Kumar[91], S. Kumar [32], S. Kundu [33], P. Kurashvili [80], A. Kurepin [142], A.B. Kurepin [142], A. Kuryakin [142], S. Kushpil [87], M.J. Kweon [59], Y. Kwon [140], S.L. La Pointe [39], P. La Rocca [27], A. Lakrathok[106], M. Lamanna [33], A.R. Landou [74,116], R. Langoy [122], P. Larionov [33], E. Laudi [33], L. Lautner [33,96], R. Lavicka [103], R. Lea [135,56], H. Lee [105], I. Legrand [46], G. Legras [127], J. Lehrbach [39], T.M. Lelek[2], R.C. Lemmon [86], I. León Monzón [110], M.M. Lesch [96], E.D. Lesser [19], P. Lévai [47], X. Li[10], X.L. Li[6], J. Lien [122], R. Lietava [101], I. Likmeta [117], B. Lim [25], S.H. Lim [17], V. Lindenstruth [39], A. Lindner[46], C. Lippmann [98], A. Liu [19], D.H. Liu [6], J. Liu [120], G.S.S. Liveraro [112], I.M. Lofnes [21], C. Loizides [88], S. Lokos [108], J. Lomker [60], P. Loncar [34], X. Lopez [128], E. López Torres [7], P. Lu [98,121], J.R. Luhder [127], M. Lunardon [28], G. Luparello [58], Y.G. Ma [40], M. Mager [33], A. Maire [130], M.V. Makariev [37], M. Malaev [142], G. Malfattore [26], N.M. Malik [92], Q.W. Malik[20], S.K. Malik [92], L. Malinina [I,VII,143], D. Mallick [132,81], N. Mallick [49], G. Mandaglio [31,54], S.K. Mandal [80], V. Manko [142], F. Manso [128], V. Manzari [51], Y. Mao [6], R.W. Marcjan [2], G.V. Margagliotti [24], A. Margotti [52], A. Marín [98], C. Markert [109], P. Martinengo [33], M.I. Martínez [45], G. Martínez García [104], M.P.P. Martins [111], S. Masciocchi [98], M. Masera [25], A. Masoni [53], L. Massacrier [132], O. Massen [60], A. Mastroserio [133,51], O. Matonoha [76], S. Mattiazzo [28], P.F.T. Matuoka[111], A. Matyja [108], C. Mayer [108], A.L. Mazuecos [33], F. Mazzaschi [25], M. Mazzilli [33], J.E. Mdhluli [124], A.F. Mechler[65], Y. Melikyan [44], A. Menchaca-Rocha [68], E. Meninno [103], A.S. Menon [117], M. Meres [13], S. Mhlanga[115,69], Y. Miake[126], L. Micheletti [33], L.C. Migliorin[129], D.L. Mihaylov [96], K. Mikhaylov [143,142], A.N. Mishra [47], D. Miśkowiec [98], A. Modak [4], A.P. Mohanty [60], B. Mohanty[81], M. Mohisin Khan [V,16], M.A. Molander [44], S. Monira [137], Z. Moravcova [84], C. Mordasini [118], D.A. Moreira De Godoy [127], I. Morozov [142], A. Morsch [33], T. Mrnjavac [33], V. Muccifora [50], S. Muhuri [136], J.D. Mulligan [75], A. Mulliri[23], M.G. Munhoz [111], R.H. Munzer [65], H. Murakami [125], S. Murray [115], L. Musa [33], J. Musinsky [61], J.W. Myrcha [137], B. Naik [124], A.I. Nambrath [19], B.K. Nandi [48], R. Nania [52], E. Nappi [51], A.F. Nassirpour [18,76], A. Nath [95], C. Nattrass [123], M.N. Naydenov [37], A. Neagu[20], A. Negru[114], L. Nellen [66], R. Nepeivoda [76], S. Nese [20], G. Neskovic [39], N. Nicassio [51], B.S. Nielsen [84], E.G. Nielsen [84], S. Nikolaev [142], S. Nikulin [142], V. Nikulin [142], F. Noferini [52], S. Noh [12], P. Nomokonov [143], J. Norman [120], N. Novitzky [126], P. Nowakowski [137], A. Nyanin [142], J. Nystrand [21], M. Ogino [77], S. Oh [18], A. Ohlson [76], V.A. Okorokov [142], J. Oleniacz [137], A.C. Oliveira Da Silva [123], M.H. Oliver [139], A. Onnerstad [118], C. Oppedisano [57], A. Ortiz Velasquez [66], J. Otwinowski [108], M. Oya[93], K. Oyama [77],

Y. Pachmayer [95], S. Padhan [48], D. Pagano [135,56], G. Paić [66], A. Palasciano [51], S. Panebianco [131], H. Park [126], H. Park [105], J. Park [59], J.E. Parkkila [33], Y. Patley [48], R.N. Patra[92], B. Paul [23], H. Pei [6], T. Peitzmann [60], X. Peng [11], M. Pennisi [25], S. Perciballi [25], D. Peresunko [142], G.M. Perez [7], Y. Pestov[142], V. Petrov [142], M. Petrovici [46], R.P. Pezzi [104,67], S. Piano [58], M. Pikna [13], P. Pillot [104], O. Pinazza [52,33], L. Pinsky[117], C. Pinto [96], S. Pisano [50], M. Płoskoń [75], M. Planinic[90], F. Pliquett[65], M.G. Poghosyan [88], B. Polichtchouk [142], S. Politano [30], N. Poljak [90], A. Pop [46], S. Porteboeuf-Houssais [128], V. Pozdniakov [143], I.Y. Pozos [45], K.K. Pradhan [49], S.K. Prasad [4], S. Prasad [49], R. Preghenella [52], F. Prino [57], C.A. Pruneau [138], I. Pshenichnov [142], M. Puccio [33], S. Pucillo [25], Z. Pugelova[107], S. Qiu [85], L. Quaglia [25], R.E. Quishpe[117], S. Ragoni [15], A. Rai [139], A. Rakotozafindrabe [131], L. Ramello [134,57], F. Rami [130], S.A.R. Ramirez [45], T.A. Rancien[74], M. Rasa [27], S.S. Räsänen [44], R. Rath [52], M.P. Rauch [21], I. Ravasenga [85], K.F. Read [88,123], C. Reckziegel [113], A.R. Redelbach [39], K. Redlich [VI,80], C.A. Reetz [98], A. Rehman[21], F. Reidt [33], H.A. Reme-Ness [35], Z. Rescakova[38], K. Reygers [95], A. Riabov [142], V. Riabov [142], R. Ricci [29], M. Richter [20], A.A. Riedel [96], W. Riegler [33], A.G. Riffero [25], C. Ristea [64], M.V. Rodriguez [33], M. Rodríguez Cahuantzi [45], K. Røed [20], R. Rogalev [142], E. Rogochaya [143], T.S. Rogoschinski [65], D. Rohr [33], D. Röhrich [21], P.F. Rojas[45], S. Rojas Torres [36], P.S. Rokita [137], G. Romanenko [26], F. Ronchetti [50], A. Rosano [31,54], E.D. Rosas[66], K. Roslon [137], A. Rossi [55], A. Roy [49], S. Roy [48], N. Rubini [26], D. Ruggiano [137], R. Rui [24], P.G. Russek [2], R. Russo [85], A. Rustamov [82], E. Ryabinkin [142], Y. Ryabov [142], A. Rybicki [108], H. Rytkonen [118], J. Ryu [17], W. Rzesa [137], O.A.M. Saarimaki [44], S. Sadhu [32], S. Sadovsky [142], J. Saetre [21], K. Šafařík [36], P. Saha[42], S.K. Saha [4], S. Saha [81], B. Sahoo [48], B. Sahoo [49], R. Sahoo [49], S. Sahoo[62], D. Sahu [49], P.K. Sahu [62], J. Saini [136], K. Sajdakova[38], S. Sakai [126], M.P. Salvan [98], S. Sambyal [92], D. Samitz [103], I. Sanna [33,96], T.B. Saramela[111], P. Sarma [42], V. Sarritzu [23], V.M. Sarti [96], M.H.P. Sas [139], J. Schambach [88], H.S. Scheid [65], C. Schiaua [46], R. Schicker [95], A. Schmah[98], C. Schmidt [98], H.R. Schmidt[94], M.O. Schmidt [33], M. Schmidt[94], N.V. Schmidt [88], A.R. Schmier [123], R. Schotter [130], A. Schröter [39], J. Schukraft [33], K. Schweda [98], G. Scioli [26], E. Scomparin [57], J.E. Seger [15], Y. Sekiguchi[125], D. Sekihata [125], M. Selina [85], I. Selyuzhenkov [98], S. Senyukov [130], J.J. Seo [95,59], D. Serebryakov [142], L. Šerkšnytė [96], A. Sevcenco [64], T.J. Shaba [69], A. Shabetai [104], R. Shahoyan[33], A. Shangaraev [142], A. Sharma[91], B. Sharma [92], D. Sharma [48], H. Sharma [55,108], M. Sharma [92], S. Sharma [77], S. Sharma [92], U. Sharma [92], A. Shatat [132], O. Sheibani[117], K. Shigaki [93], M. Shimomura[78], J. Shin[12], S. Shirinkin [142], Q. Shou [40], Y. Sibiriak [142], S. Siddhanta [53], T. Siemiarczuk [80], T.F. Silva [111], D. Silvermyr [76], T. Simantathammakul[106], R. Simeonov [37], B. Singh[92], B. Singh [96], K. Singh [49], R. Singh [81], R. Singh [92], R. Singh [49], S. Singh [16], V.K. Singh [136], V. Singhal [136], T. Sinha [100], B. Sitar [13], M. Sitta [134,57], T.B. Skaali[20], G. Skorodumovs [95], M. Slupecki [44], N. Smirnov [139], R.J.M. Snellings [60], E.H. Solheim [20], J. Song [117], A. Songmoolnak[106], C. Sonnabend [33,98], F. Soramel [28], A.B. Soto-hernandez [89], R. Spijkers [85], I. Sputowska [108], J. Staa [76], J. Stachel [95], I. Stan [64], P.J. Steffanic [123], S.F. Stiefelmaier [95], D. Stocco [104], I. Storehaug [20], P. Stratmann [127], S. Strazzi [26], A. Sturniolo [31,54], C.P. Stylianidis[85], A.A.P. Suaide [111], C. Suire [132], M. Sukhanov [142], M. Suljic [33], R. Sultanov [142], V. Sumberia [92], S. Sumowidagdo [83], S. Swain[62], I. Szarka [13], M. Szymkowski [137], S.F. Taghavi [96], G. Taillepied [98], J. Takahashi [112], G.J. Tambave [81], S. Tang [6], Z. Tang [121], J.D. Tapia Takaki [119], N. Tapus[114], L.A. Tarasovicova [127], M.G. Tarzila [46], G.F. Tassielli [32], A. Tauro [33], G. Tejeda Muñoz [45], A. Telesca [33], L. Terlizzi [25], C. Terrevoli [117], S. Thakur [4], D. Thomas [109], A. Tikhonov [142], A.R. Timmins [117], M. Tkacik[107], T. Tkacik [107], A. Toia [65], R. Tokumoto[93], K. Tomohiro[93], N. Topilskaya [142], M. Toppi [50], T. Tork [132], V.V. Torres [104], A.G. Torres Ramos [32], A. Trifiró [31,54], A.S. Triolo [33,31,54], S. Tripathy [52], T. Tripathy [48], S. Trogolo [33], V. Trubnikov [3], W.H. Trzaska [118], T.P. Trzcinski [137], A. Tumkin [142], R. Turrisi [55], T.S. Tveter [20], K. Ullaland [21], B. Ulukutlu [96], A. Uras [129], G.L. Usai [23], M. Vala[38], N. Valle [22], L.V.R. van Doremalen[60], M. van Leeuwen [85], C.A. van Veen [95], R.J.G. van Weelden [85], P. Vande Vyvre [33], D. Varga [47], Z. Varga [47], M. Vasileiou [79], A. Vasiliev [142], O. Vázquez Doce [50], O. Vazquez Rueda [117], V. Vechernin [142], E. Vercellin [25], S. Vergara Limón[45], R. Verma[48], L. Vermunt [98], R. Vértesi [47], M. Verweij [60], L. Vickovic[34], Z. Vilakazi[124], O. Villalobos Baillie [101], A. Villani [24], G. Vino [51], A. Vinogradov [142], T. Virgili [29], M.M.O. Virta [118], V. Vislavicius[76], A. Vodopyanov [143], B. Volkel [33], M.A. Völkl [95], K. Voloshin[142], S.A. Voloshin [138], G. Volpe [32], B. von Haller [33], I. Vorobyev [96], N. Vozniuk [142], J. Vrláková [38], J. Wan[40], C. Wang [40], D. Wang[40], Y. Wang [40], Y. Wang [6], A. Wegrzynek [33], F.T. Weiglhofer[39], S.C. Wenzel [33], J.P. Wessels [127], S.L. Weyhmiller [139], J. Wiechula [65], J. Wikne [20], G. Wilk [80], J. Wilkinson [98], G.A. Willems [127], B. Windelband [95],

M. Winn [131], J.R. Wright [109], W. Wu[40], Y. Wu [121], R. Xu [6], A. Yadav [43], A.K. Yadav [136], S. Yalcin [73], Y. Yamaguchi [93], S. Yang[21], S. Yano [93], Z. Yin [6], I.-K. Yoo [17], J.H. Yoon [59], H. Yu[12], S. Yuan[21], A. Yuncu [95], V. Zaccolo [24], C. Zampolli [33], F. Zanone [95], N. Zardoshti [33], A. Zarochentsev [142], P. Závada [63], N. Zaviyalov[142], M. Zhalov [142], B. Zhang [6], C. Zhang [131], L. Zhang [40], S. Zhang [40], X. Zhang [6], Y. Zhang[121], Z. Zhang [6], M. Zhao [10], V. Zherebchevskii [142], Y. Zhi[10], D. Zhou [6], Y. Zhou [84], J. Zhu [98,6], Y. Zhu[6], S.C. Zugravel [57], N. Zurlo [135,56]

Affiliation Notes

[I] Deceased
[II] Also at: Max-Planck-Institut fur Physik, Munich, Germany
[III] Also at: Italian National Agency for New Technologies, Energy and Sustainable Economic Development (ENEA), Bologna, Italy
[IV] Also at: Dipartimento DET del Politecnico di Torino, Turin, Italy
[V] Also at: Department of Applied Physics, Aligarh Muslim University, Aligarh, India
[VI] Also at: Institute of Theoretical Physics, University of Wroclaw, Poland
[VII] Also at: An institution covered by a cooperation agreement with CERN

Collaboration Institutes

[1] A.I. Alikhanyan National Science Laboratory (Yerevan Physics Institute) Foundation, Yerevan, Armenia
[2] AGH University of Krakow, Cracow, Poland
[3] Bogolyubov Institute for Theoretical Physics, National Academy of Sciences of Ukraine, Kiev, Ukraine
[4] Bose Institute, Department of Physics and Centre for Astroparticle Physics and Space Science (CAPSS), Kolkata, India
[5] California Polytechnic State University, San Luis Obispo, California, United States
[6] Central China Normal University, Wuhan, China
[7] Centro de Aplicaciones Tecnológicas y Desarrollo Nuclear (CEADEN), Havana, Cuba
[8] Centro de Investigación y de Estudios Avanzados (CINVESTAV), Mexico City and Mérida, Mexico
[9] Chicago State University, Chicago, Illinois, United States
[10] China Institute of Atomic Energy, Beijing, China
[11] China University of Geosciences, Wuhan, China
[12] Chungbuk National University, Cheongju, Republic of Korea
[13] Comenius University Bratislava, Faculty of Mathematics, Physics and Informatics, Bratislava, Slovak Republic
[14] COMSATS University Islamabad, Islamabad, Pakistan
[15] Creighton University, Omaha, Nebraska, United States
[16] Department of Physics, Aligarh Muslim University, Aligarh, India
[17] Department of Physics, Pusan National University, Pusan, Republic of Korea
[18] Department of Physics, Sejong University, Seoul, Republic of Korea
[19] Department of Physics, University of California, Berkeley, California, United States
[20] Department of Physics, University of Oslo, Oslo, Norway
[21] Department of Physics and Technology, University of Bergen, Bergen, Norway
[22] Dipartimento di Fisica, Università di Pavia, Pavia, Italy
[23] Dipartimento di Fisica dell'Università and Sezione INFN, Cagliari, Italy
[24] Dipartimento di Fisica dell'Università and Sezione INFN, Trieste, Italy
[25] Dipartimento di Fisica dell'Università and Sezione INFN, Turin, Italy
[26] Dipartimento di Fisica e Astronomia dell'Università and Sezione INFN, Bologna, Italy
[27] Dipartimento di Fisica e Astronomia dell'Università and Sezione INFN, Catania, Italy
[28] Dipartimento di Fisica e Astronomia dell'Università and Sezione INFN, Padova, Italy
[29] Dipartimento di Fisica 'E.R. Caianiello' dell'Università and Gruppo Collegato INFN, Salerno, Italy
[30] Dipartimento DISAT del Politecnico and Sezione INFN, Turin, Italy
[31] Dipartimento di Scienze MIFT, Università di Messina, Messina, Italy
[32] Dipartimento Interateneo di Fisica 'M. Merlin' and Sezione INFN, Bari, Italy
[33] European Organization for Nuclear Research (CERN), Geneva, Switzerland
[34] Faculty of Electrical Engineering, Mechanical Engineering and Naval Architecture, University of Split, Split, Croatia

[35] Faculty of Engineering and Science, Western Norway University of Applied Sciences, Bergen, Norway
[36] Faculty of Nuclear Sciences and Physical Engineering, Czech Technical University in Prague, Prague, Czech Republic
[37] Faculty of Physics, Sofia University, Sofia, Bulgaria
[38] Faculty of Science, P.J. Šafárik University, Košice, Slovak Republic
[39] Frankfurt Institute for Advanced Studies, Johann Wolfgang Goethe-Universität Frankfurt, Frankfurt, Germany
[40] Fudan University, Shanghai, China
[41] Gangneung-Wonju National University, Gangneung, Republic of Korea
[42] Gauhati University, Department of Physics, Guwahati, India
[43] Helmholtz-Institut für Strahlen- und Kernphysik, Rheinische Friedrich-Wilhelms-Universität Bonn, Bonn, Germany
[44] Helsinki Institute of Physics (HIP), Helsinki, Finland
[45] High Energy Physics Group, Universidad Autónoma de Puebla, Puebla, Mexico
[46] Horia Hulubei National Institute of Physics and Nuclear Engineering, Bucharest, Romania
[47] HUN-REN Wigner Research Centre for Physics, Budapest, Hungary
[48] Indian Institute of Technology Bombay (IIT), Mumbai, India
[49] Indian Institute of Technology Indore, Indore, India
[50] INFN, Laboratori Nazionali di Frascati, Frascati, Italy
[51] INFN, Sezione di Bari, Bari, Italy
[52] INFN, Sezione di Bologna, Bologna, Italy
[53] INFN, Sezione di Cagliari, Cagliari, Italy
[54] INFN, Sezione di Catania, Catania, Italy
[55] INFN, Sezione di Padova, Padova, Italy
[56] INFN, Sezione di Pavia, Pavia, Italy
[57] INFN, Sezione di Torino, Turin, Italy
[58] INFN, Sezione di Trieste, Trieste, Italy
[59] Inha University, Incheon, Republic of Korea
[60] Institute for Gravitational and Subatomic Physics (GRASP), Utrecht University/Nikhef, Utrecht, Netherlands
[61] Institute of Experimental Physics, Slovak Academy of Sciences, Košice, Slovak Republic
[62] Institute of Physics, Homi Bhabha National Institute, Bhubaneswar, India
[63] Institute of Physics of the Czech Academy of Sciences, Prague, Czech Republic
[64] Institute of Space Science (ISS), Bucharest, Romania
[65] Institut für Kernphysik, Johann Wolfgang Goethe-Universität Frankfurt, Frankfurt, Germany
[66] Instituto de Ciencias Nucleares, Universidad Nacional Autónoma de México, Mexico City, Mexico
[67] Instituto de Física, Universidade Federal do Rio Grande do Sul (UFRGS), Porto Alegre, Brazil
[68] Instituto de Física, Universidad Nacional Autónoma de México, Mexico City, Mexico
[69] iThemba LABS, National Research Foundation, Somerset West, South Africa
[70] Jeonbuk National University, Jeonju, Republic of Korea
[71] Johann-Wolfgang-Goethe Universität Frankfurt Institut für Informatik, Fachbereich Informatik und Mathematik, Frankfurt, Germany
[72] Korea Institute of Science and Technology Information, Daejeon, Republic of Korea
[73] KTO Karatay University, Konya, Turkey
[74] Laboratoire de Physique Subatomique et de Cosmologie, Université Grenoble-Alpes, CNRS-IN2P3, Grenoble, France
[75] Lawrence Berkeley National Laboratory, Berkeley, California, United States
[76] Lund University Department of Physics, Division of Particle Physics, Lund, Sweden
[77] Nagasaki Institute of Applied Science, Nagasaki, Japan
[78] Nara Women's University (NWU), Nara, Japan
[79] National and Kapodistrian University of Athens, School of Science, Department of Physics , Athens, Greece
[80] National Centre for Nuclear Research, Warsaw, Poland
[81] National Institute of Science Education and Research, Homi Bhabha National Institute, Jatni, India
[82] National Nuclear Research Center, Baku, Azerbaijan
[83] National Research and Innovation Agency - BRIN, Jakarta, Indonesia
[84] Niels Bohr Institute, University of Copenhagen, Copenhagen, Denmark
[85] Nikhef, National institute for subatomic physics, Amsterdam, Netherlands
[86] Nuclear Physics Group, STFC Daresbury Laboratory, Daresbury, United Kingdom

[87] Nuclear Physics Institute of the Czech Academy of Sciences, Husinec-Řež, Czech Republic
[88] Oak Ridge National Laboratory, Oak Ridge, Tennessee, United States
[89] Ohio State University, Columbus, Ohio, United States
[90] Physics department, Faculty of science, University of Zagreb, Zagreb, Croatia
[91] Physics Department, Panjab University, Chandigarh, India
[92] Physics Department, University of Jammu, Jammu, India
[93] Physics Program and International Institute for Sustainability with Knotted Chiral Meta Matter (SKCM2), Hiroshima University, Hiroshima, Japan
[94] Physikalisches Institut, Eberhard-Karls-Universität Tübingen, Tübingen, Germany
[95] Physikalisches Institut, Ruprecht-Karls-Universität Heidelberg, Heidelberg, Germany
[96] Physik Department, Technische Universität München, Munich, Germany
[97] Politecnico di Bari and Sezione INFN, Bari, Italy
[98] Research Division and ExtreMe Matter Institute EMMI, GSI Helmholtzzentrum für Schwerionenforschung GmbH, Darmstadt, Germany
[99] Saga University, Saga, Japan
[100] Saha Institute of Nuclear Physics, Homi Bhabha National Institute, Kolkata, India
[101] School of Physics and Astronomy, University of Birmingham, Birmingham, United Kingdom
[102] Sección Física, Departamento de Ciencias, Pontificia Universidad Católica del Perú, Lima, Peru
[103] Stefan Meyer Institut für Subatomare Physik (SMI), Vienna, Austria
[104] SUBATECH, IMT Atlantique, Nantes Université, CNRS-IN2P3, Nantes, France
[105] Sungkyunkwan University, Suwon City, Republic of Korea
[106] Suranaree University of Technology, Nakhon Ratchasima, Thailand
[107] Technical University of Košice, Košice, Slovak Republic
[108] The Henryk Niewodniczanski Institute of Nuclear Physics, Polish Academy of Sciences, Cracow, Poland
[109] The University of Texas at Austin, Austin, Texas, United States
[110] Universidad Autónoma de Sinaloa, Culiacán, Mexico
[111] Universidade de São Paulo (USP), São Paulo, Brazil
[112] Universidade Estadual de Campinas (UNICAMP), Campinas, Brazil
[113] Universidade Federal do ABC, Santo Andre, Brazil
[114] Universitatea Nationala de Stiinta si Tehnologie Politehnica Bucuresti, Bucharest, Romania
[115] University of Cape Town, Cape Town, South Africa
[116] University of Derby, Derby, United Kingdom
[117] University of Houston, Houston, Texas, United States
[118] University of Jyväskylä, Jyväskylä, Finland
[119] University of Kansas, Lawrence, Kansas, United States
[120] University of Liverpool, Liverpool, United Kingdom
[121] University of Science and Technology of China, Hefei, China
[122] University of South-Eastern Norway, Kongsberg, Norway
[123] University of Tennessee, Knoxville, Tennessee, United States
[124] University of the Witwatersrand, Johannesburg, South Africa
[125] University of Tokyo, Tokyo, Japan
[126] University of Tsukuba, Tsukuba, Japan
[127] Universität Münster, Institut für Kernphysik, Münster, Germany
[128] Université Clermont Auvergne, CNRS/IN2P3, LPC, Clermont-Ferrand, France
[129] Université de Lyon, CNRS/IN2P3, Institut de Physique des 2 Infinis de Lyon, Lyon, France
[130] Université de Strasbourg, CNRS, IPHC UMR 7178, F-67000 Strasbourg, France, Strasbourg, France
[131] Université Paris-Saclay, Centre d'Etudes de Saclay (CEA), IRFU, Départment de Physique Nucléaire (DPhN), Saclay, France
[132] Université Paris-Saclay, CNRS/IN2P3, IJCLab, Orsay, France
[133] Università degli Studi di Foggia, Foggia, Italy
[134] Università del Piemonte Orientale, Vercelli, Italy
[135] Università di Brescia, Brescia, Italy
[136] Variable Energy Cyclotron Centre, Homi Bhabha National Institute, Kolkata, India
[137] Warsaw University of Technology, Warsaw, Poland
[138] Wayne State University, Detroit, Michigan, United States
[139] Yale University, New Haven, Connecticut, United States

[140] Yonsei University, Seoul, Republic of Korea
[141] Zentrum für Technologie und Transfer (ZTT), Worms, Germany
[142] Affiliated with an institute covered by a cooperation agreement with CERN
[143] Affiliated with an international laboratory covered by a cooperation agreement with CERN.